

# Synthesis of a New Class of 1,4-Bis(diphenylphosphino)-1,3-butadiene Bridged Diphosphine, NUPHOS, via Zirconium-Mediated Reductive Coupling of Alkynes and Diynes: Applications in Palladium-Catalyzed Cross-Coupling Reactions

Simon Doherty,<sup>\*,†,‡</sup> Edward G. Robins,<sup>†</sup> Mark Nieuwenhuyzen,<sup>†</sup>  
Julian G. Knight,<sup>\*,§</sup> Paul A. Champkin,<sup>§</sup> and William Clegg<sup>§</sup>

*School of Chemistry, David Keir Building, The Queen's University of Belfast, Stranmillis Roads, Belfast BT9 5AG, United Kingdom, and Department of Chemistry, Bedson Building, University of Newcastle, Newcastle upon Tyne NE1 7RU, United Kingdom*

*Received December 11, 2001*

Zirconium-mediated inter- and intramolecular reductive cyclization of alkynes and diynes has been used to prepare a new class of bidentate phosphine, based on a four-carbon  $sp^2$ -hybridized tether. Intermolecular coupling of diphenylacetylene and but-2-yne with Negishi's reagent followed by transmetalation with copper chloride prior to quenching with chlorodiphenylphosphine affords the corresponding acyclic diphosphines 1,4-bis(diphenylphosphino)-1,2,3,4-tetraphenyl-1,3-butadiene (**2a**; 1,2,3,4- $Ph_4$ -NUPHOS) and 1,4-bis(diphenylphosphino)-1,2,3,4-tetramethyl-1,3-butadiene (**2b**; 1,2,3,4- $Me_4$ -NUPHOS), respectively. A single-crystal X-ray analysis of the former has been obtained. Surprisingly, 1-phenylpropyne undergoes a highly regioselective reductive cyclization to afford 1,4-bis(diphenylphosphino)-1,3-diphenyl-2,4-dimethyl-1,3-butadiene (**2c**; 1,3- $Ph_2$ -2,4- $Me_2$ -NUPHOS). Similarly, transmetalation of the zirconacyclopentadiene generated from 3,9-dodecadiyne and 1,8-diphenyloctadiyne followed by electrophilic liberation of the resulting copper diene reagent with chlorodiphenylphosphine gave 1,2-bis(1-(diphenylphosphino)prop-1-ylidene)cyclohexane (**2d**; 1,4- $Et_2$ -2,3-cyclo- $C_6H_8$ -NUPHOS) and 1,2-bis(1-(diphenylphosphino)benzylidene)cyclohexane (**2e**; 1,4- $Ph_2$ -2,3-cyclo- $C_6H_8$ -NUPHOS), respectively. This methodology provides a convenient and versatile one-pot synthesis of a wide range of 1,3-diene bridged diphosphines. Single-crystal X-ray analyses of [(1,2,3,4- $Ph_4$ -NUPHOS) $PdCl_2$ ], [(1,3- $Ph_2$ -2,4- $Me_2$ -NUPHOS) $PdCl_2$ ], and [(1,4- $Ph_2$ -2,3-cyclo- $C_6H_8$ -NUPHOS) $PtCl_2$ ] reveal that these new phosphines coordinate to palladium and platinum in much the same manner as BINAP and dpbp, with a significant torsional twist about the C(2)–C(3) bond of the backbone. The copper diphosphine intermediate [Cu(1,4- $Et_2$ -2,3-cyclo- $C_6H_8$ -NUPHOS)Cl]<sub>2</sub> (**1d**) has also been isolated and characterized by single-crystal X-ray analysis and exists as the chloro-bridged dimer in which the 1,2-bis(1-(diphenylphosphino)prop-1-ylidene)cyclohexane coordinates in a bidentate manner. Palladium complexes of these new diphosphines are highly active for the cross-coupling of bromobenzene and *sec*-butylmagnesium bromide. Catalyst mixtures based on 1,2,3,4- $Ph_4$ -NUPHOS are far superior to those based on BINAP, with activities of 6900 and 260 (mol of product) (mol of palladium)<sup>–1</sup> h<sup>–1</sup>, respectively. In fact, catalysts based on 1,2,3,4- $Ph_4$ -NUPHOS are ~30 times more active than the most active catalyst reported to date for this coupling. In comparison, the selectivity of the corresponding cross-coupling with 2-bromopropene depends markedly on the nature of the NUPHOS derivative. In general, those based on NUPHOS derivatives with acyclic tethers, namely **2a–c**, are highly selective for the formation of 2,3-dimethylpentene, while those formed from **2d,e** gave a mixture of 2,3-dimethylpentene, 2-methylhexene, and 2,3-dimethylbutadiene. The initial TOF, measured after 20 min, also shows a marked variation on the nature of the phosphine and while all NUPHOS-based catalysts outperform those based on BINAP, catalyst mixtures based on dpfp showed both high selectivity (>99%) and impressive activity. Mixtures of  $Pd_2$ -(dba)<sub>3</sub> and the NUPHOS derivatives **2a–e** also catalyze the Suzuki cross-coupling of bromobenzene and 4-bromoacetophenone with phenyl boronic acid, with conversions up to 100% at catalyst loadings as low as 0.0001 mol % Pd (TON =  $1 \times 10^6$ ).

## Introduction

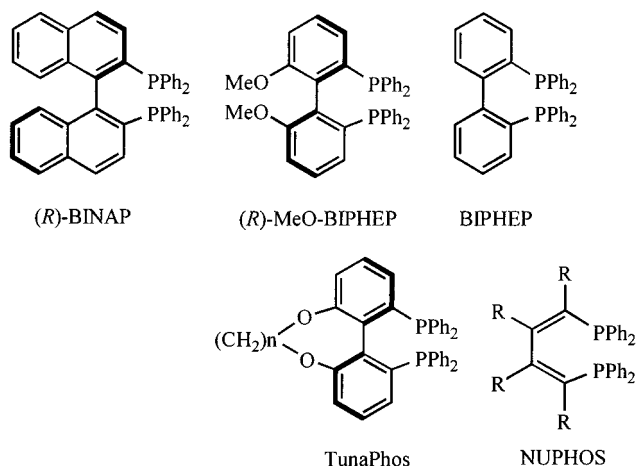
The discovery that transition-metal complexes of 2,2'-bis(diphenylphosphino)-1,1'-binaphthyl (BINAP) catalyze a wide range of asymmetric transformations, often with spectacular efficiency, was a landmark discovery

in homogeneous catalysis with immense potential for performing key steps in the synthesis of important organic compounds.<sup>1</sup> Transfer of chirality in BINAP-based transformations, such as stereoselective hydrogenation, relies on the formation of a highly skewed seven-membered chelate ring. The atropisomerism of BINAP fixes the conformation of this ring and determines the spatial arrangement of the chiral P-phenyl rings, which ulti-

<sup>†</sup> The Queen's University of Belfast.

<sup>‡</sup> E-mail: s.doherty@qub.ac.uk.

<sup>§</sup> University of Newcastle. E-mail (J.G.K.): j.g.knight@ncl.ac.uk.



mately exert steric influence on the substrate binding sites.

The success of BINAP and its derivatives has prompted investigations into the development and applications of alternative structurally related biaryl atropisomeric diphosphines,<sup>2</sup> often based on a 6,6'-substituted biphenyl tether such as (*R*)-MeO-BIPHEP and (*R*)-BIPHEP (the 6,6'-substituents are OMe and Me, respectively).<sup>3</sup> These ligands have several features in common with BINAP in that they are bidentate triarylphosphines with two diphenylphosphino groups bridged by an sp<sup>2</sup>-hybridized four-carbon tether which form a skewed seven-membered chelate ring when coordinated to a metal center. Schmid and co-workers have prepared over 60 such derivatives and investigated the influence of steric and electronic properties on the enantioselectivity and rates of hydrogenation of unconventional substrates, including  $\alpha$ -pyridyl ketones,  $\gamma$ -keto olefins, an  $\alpha$ -pyrone, and an enol ether of a  $\beta$ -keto lactam.<sup>4</sup> MeO-BIPHEP-based diphosphines with  $\alpha$ -furyl and 3,5-di-*tert*-butylphenyl substituents attached to phosphorus were shown to form particularly effective catalysts, giving ee's in excess of 95%. Pregosin has since shown that the 3,5-di-*tert*-butylphenyl-substituted derivative affects the asymmetric palladium-catalyzed Heck reaction and allylic alkylation with enantioselectivities of >98% and 90%, respectively,<sup>5</sup> and has attributed this efficiency to the 3,5-dialkylmetal effect, the combination

of a more rigid and slightly larger chiral pocket, as compared to that formed by MeO-BIPHEP. In contrast to BINAP, MeO-BIPHEP is also capable of acting as a six-electron donor to Ru(II), via coordination of one of the biaryl double bonds, and these complexes catalyze the regiospecific addition of carboxylic acids to terminal alkynes, to give the corresponding enol esters.<sup>6</sup> Variation of the dihedral angle in a series of closely related MeO-BIPHEP type diphosphines, TunaPhos, has revealed that the ruthenium-catalyzed enantioselective hydrogenation of  $\beta$ -keto esters depends markedly on the bite angle and reaches a maximum at 88°. <sup>7</sup> The enantioselectivities obtained in the ruthenium-catalyzed asymmetric hydrogenation of  $\beta$ -keto esters using the atropisomeric 3,3'-dipyridyldiphosphine 2,2',6,6'-tetramethoxy-4,4'-bis(diphenylphosphino)-3,3'-bipyridine (P-phos) compare favorably with Ru(BINAP) systems, with the advantage of facile catalyst separation by extraction with aqueous hydrochloric acid.<sup>8</sup>

For reactions that do not involve an asymmetric transformation, it would be more practical to use an alternative, less expensive, but structurally similar diphosphine: for example, 2,2'-bis(diphenylphosphino)-1,1'-biphenyl (BIPHEP).<sup>9</sup> In this regard, Hayashi and co-workers have recently shown that the selectivity of BIPHEP-based complexes in the palladium-catalyzed cross-coupling of *sec*-BuMgCl with vinyl halides is higher than that achieved with palladium catalysts of 1,2-bis(diphenylphosphino)ethane (dppe) and comparable to that obtained using 1,1'-bis(diphenylphosphino)-ferrocene (dppf).<sup>10</sup> This ligand has also been applied to the rhodium-catalyzed Michael addition of boronic acids to enones and the palladium-catalyzed amination of aryl bromides, the former showing activities far superior to those of the corresponding catalyst based on 1,4-bis(diphenylphosphino)butane (dppb). In an independent report, Noyori has shown that activation of ruthenium complexes of BIPHEP, with an appropriate chiral amine such as (*S,S*)-1,2-diphenylethylenediamine ((*S,S*)-DPEN), results in the highly enantioselective hydrogenation of carbonyl compounds,<sup>11</sup> further highlighting the potential utility of this ligand type.

Given the effectiveness of biphenyl-based diphosphines and their potential impact in platinum group catalysis, there is likely to be considerable interest in the development of new methodology for the synthesis of related diphosphines. In this regard, we have recently utilized the zirconium-mediated reductive cyclization of alkynes to prepare a new class of diphosphine, NUPHOS.<sup>12</sup> Some time ago Fagan and co-workers demonstrated that zirconacyclopentadienes react with

(1) (a) Noyori, R. *Asymmetric Catalysis in Organic Synthesis*; Wiley: New York, 1994. (b) Noyori, R.; Takaya, H. *Acc. Chem. Res.* **1990**, *23*, 345. (c) Miyashita, A.; Yasuda, A.; Takaya, K.; Torumi, T.; Ita, T.; Sauchi, T.; Noyori, R. *J. Am. Chem. Soc.* **1980**, *102*, 7933. (d) Cho, S. Y.; Shibasaki, M. *Tetrahedron Lett.* **1998**, *39*, 1773. (e) Ozawa, F.; Kubo, A.; Hayashi, T. *J. Am. Chem. Soc.* **1991**, *113*, 1417. (f) Shibasaki, M.; Boden, C. D. L.; Kojima, A. *Tetrahedron* **1997**, *53*, 7371. (g) Wolfe, T. P.; Wagaw, S.; Buchwald, S. L. *J. Am. Chem. Soc.* **1996**, *118*, 7215.

(2) For selected examples see: (a) Andersen, N. G.; McDonald, R.; Keay, B. A. *Tetrahedron: Asymmetry* **2001**, *12*, 263. (b) Tietze, L. F.; Thede, K.; Schimpf, R.; Sannicola, F. *Chem. Commun.* **2000**, 583. (c) Tietze, L. F.; Thede, K.; Sannicola, F. *Chem. Commun.* **1999**, 1811. (d) Benincori, T.; Brenna, E.; Sannicola, F.; Trimarco, L.; Antognazza, P.; Cesarotti, E.; Demartin, F.; Pilati, T. *J. Org. Chem.* **1996**, *61*, 6244. (e) Berens, V.; Brown, J.; Long, J.; Selke, R. *Tetrahedron: Asymmetry* **1996**, *7*, 285. (f) Cereghetti, M.; Arnold, W.; Broger, E. A.; Rageot, A. *Tetrahedron Lett.* **1996**, *37*, 5347. (g) Heisser, B.; Broger, E. A.; Cramer, Y. *Tetrahedron: Asymmetry* **1991**, *2*, 51.

(3) (a) Schmid, R.; Firicher, J.; Cereghetti, M.; Schonholzer, P. *Helv. Chim. Acta* **1991**, *74*, 370. (b) Schmid, R.; Cereghetti, M.; Schonholzer, P.; Hansen, H.-J. *Helv. Chim. Acta* **1988**, *71*, 897.

(4) (a) Fehr, M. J.; Consiglio, G.; Scalone, M.; Schmid, R. *J. Org. Chem.* **1999**, *64*, 5768. (b) Schmid, R.; Broger, E.; Cereghetti, M.; Cramer, Y.; Foricher, J.; Lalonde, M.; Muller, R. K.; Scalone, M.; Schoettl, G.; Zutter, U. *Pure Appl. Chem.* **1996**, *68*, 131.

(5) Trabesinger, G.; Albinati, A.; Feiken, N.; Kunz, R. W.; Pregosin, P. S.; Tschoerner, M. *J. Am. Chem. Soc.* **1997**, *119*, 6315.

(6) den Reijer, C. J.; Drago, D.; Pregosin, P. S. *Organometallics* **2001**, *20*, 2982.

(7) Zhang, Z.; Qian, H.; Longmire, J.; Zhang, X. *J. Org. Chem.* **2000**, *65*, 6223.

(8) Pai, C.-C.; Lin, C.-W.; Lin, C.-C.; Chen, C.-C.; Chan, A. S. C. *J. Am. Chem. Soc.* **2000**, *122*, 11513.

(9) (a) Desponds, O.; Schlosser, M. *J. Organomet. Chem.* **1996**, *507*, 257. (b) Desponds, O.; Schlosser, M. *Tetrahedron Lett.* **1996**, *37*, 47.

(10) Ogasawara, M.; Yoshida, K.; Hayashi, T. *Organometallics* **2000**, *19*, 1567.

(11) (a) Mikami, K.; Korenaga, T.; Terada, M.; Ohkuma, T.; Pham, T.; Noyori, R. *Angew. Chem., Int. Ed.* **1999**, *38*, 495. (b) Badur-Rashid, K.; Faatz, M.; Lough, A. J.; Morris, R. H. *J. Am. Chem. Soc.* **2001**, *123*, 7473.

(12) Doherty, S.; Knight, J. G.; Robins, E. G.; Scanlan, T. H.; Champkin, P. A.; Clegg, W. *J. Am. Chem. Soc.* **2001**, *123*, 5110.

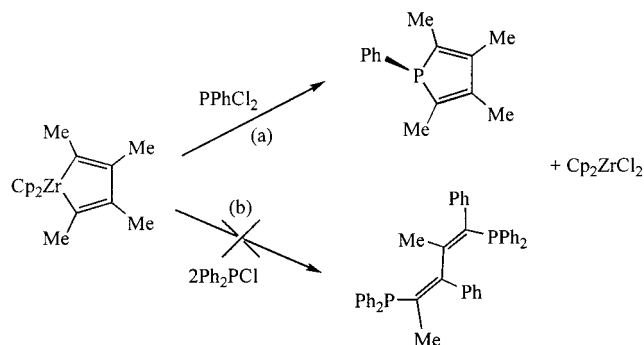
electrophilic reagents to liberate the corresponding main-group heterocycle, in the case of dichlorophenylphosphine to give the 1-phenyl-2,3,4,5-tetrasubstituted phosphole.<sup>13</sup> We have been investigating the synthesis of bidentate phosphines using this route and have recently reported that treatment of the zirconacyclopentadiene formed from diphenylacetylene with 2 equiv of chlorodiphenylphosphine affords 1,4-bis(diphenylphosphino)-1,2,3,4-tetraphenyl-1,3-butadiene (1,2,3,4-Ph<sub>4</sub>-NUPHOS) in high yield, noting that the success of this reaction relied on the presence of a stoichiometric amount of copper chloride. In comparing the structures of NUPHOS, BINAP, BIPHEP, and MeO-BIPHEP, there is a clear similarity between the basic skeletal frameworks of these diphosphines in that they all contain two diphenylphosphino groups connected by an sp<sup>2</sup>-hybridized four-carbon tether. We see this as a particularly attractive methodology for the synthesis of diphosphines since (i) it is a relatively straightforward procedure that can be carried out in a single pot, (ii) it offers immense scope for structural variation, and hence catalyst tuning, since a wide range of alkynes and diynes are known to undergo reductive cyclization by Negishi's reagent, and (iii) the ready availability of chiral diynes lends this methodology to the synthesis of chiral diphosphines.

Preliminary catalyst testing has revealed that palladium complexes of this new class of diphosphine are highly active for the cross-coupling of *sec*-butylmagnesium bromide with bromobenzene. Herein we describe full details of the use of inter- and intramolecular reductive cyclization of alkynes and diynes to synthesize an entirely new class of 1,3-butadiene bridged diphosphine, the structures of several palladium and platinum complexes of these diphosphines, and the results of palladium-catalyzed Grignard cross-coupling and Suzuki cross-coupling reactions. The results of our preliminary studies have appeared in the form of a communication.<sup>12</sup>

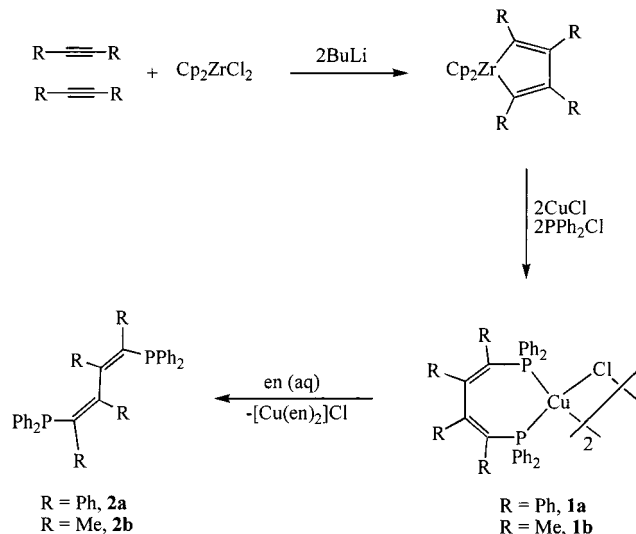
## Results and Discussion

**Synthesis and Characterization of NUPHOS-Type Diphosphines (2a–e).** Some time ago Fagan demonstrated that zirconacyclopentadienes, generated either via intermolecular coupling of alkynes or intramolecular coupling of diynes, readily react with dichlorophenylphosphine via metallacycle transfer from zirconium to afford the corresponding 1-phenylphosphole (Scheme 1a). We reasoned that treatment of such zirconacyclopentadienes with chlorodiphenylphosphine should liberate the corresponding substituted 1,4-bis(diphenylphosphino)-1,3-dienes according to Scheme 1b. Unfortunately, we have been unable to isolate any phosphorus-containing compounds from the reaction of chlorodiphenylphosphine with a deep red solution of the zirconacyclopentadiene, generated in situ from Negishi's reagent and 2 equiv of diphenylacetylene or but-2-yne. Remarkably, though, transmetalation of the zirconacyclopentadiene with copper chloride prior to addition of chlorodiphenylphosphine resulted in a rapid and clean reaction to give the desired diphosphine **2a,b**, as an

**Scheme 1**



**Scheme 2**



intensely colored copper complex. The <sup>31</sup>P{<sup>1</sup>H} spectra of these intermediate copper complexes contain a single broad resonance at δ -4.3 and -0.9 for **2a** and **2b**, respectively, with a half-height line width (Δν<sub>1/2</sub>) of ca. 250 Hz.

To fully characterize this new class of diphosphine, examine their coordination chemistry, and undertake catalyst testing, **2a,b** must first be liberated from the copper, a process that is readily accomplished by repeated extraction of a dichloromethane or diethyl ether/tetrahydrofuran solution with either aqueous ammonia or ethylenediamine, until the washings no longer exhibit a blue coloration on exposure to oxygen (Scheme 2). In each case the diphosphine is isolated as an off-white, relatively air stable solid which can be recrystallized from an appropriate solvent. The <sup>31</sup>P{<sup>1</sup>H} NMR spectra of **2a** and **2b** contain a single sharp resonance at δ 1.1 and -4.2, respectively, the former shifted slightly downfield of that corresponding to its copper complex.

Transmetalation of the zirconium-carbon(sp<sup>2</sup>) bond to copper is essential for the formation of these diphosphines. In this regard, Takahashi has recently shown that the α-substituted zirconocenes [Cp<sub>2</sub>Zr(OSiMe<sub>3</sub>)-{C(R)=C(R)CH<sub>2</sub>CH=CH<sub>2</sub>}] (R = Pr, Ph) do not react with chlorodiphenylphosphine, even at elevated temperatures and that addition of copper chloride to the reaction mixture is necessary to ensure formation of the tethered olefin phosphine complex [Cu{PR<sub>2</sub>C(H)=C(H)-CH<sub>2</sub>CH=CH<sub>2</sub>}Cl]<sub>2</sub> via P-C bond formation.<sup>14</sup> While transfer of an sp<sup>2</sup> carbon from zirconium to an electro-

(13) (a) Fagan, P. J.; Nugent, W. A. *J. Am. Chem. Soc.* **1988**, *110*, 2310. (b) Fagan, P. J.; Nugent, W. A.; Calabrese, J. C. *J. Am. Chem. Soc.* **1994**, *116*, 1880.

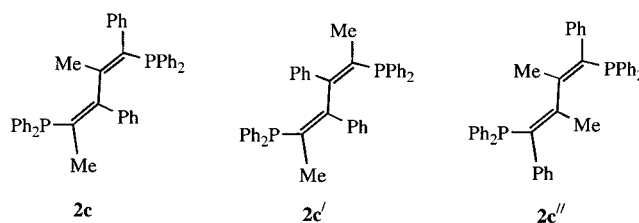


philic aryl-substituted chlorophosphine appears to require a copper-mediated transmetalation, zirconacyclopentanes and zirconacyclopentenes have been shown to react with chlorodiphenylphosphine to liberate alkylphosphines and homoallylic phosphines, respectively, via selective activation of the Zr–C(sp<sup>3</sup>) bond.<sup>15</sup> In the case of zirconacyclopentanes, the first Zr–C(sp<sup>3</sup>) bond reacts rapidly with PPh<sub>2</sub>Cl to give the corresponding monophosphine as the major product together with minor amounts of the desired diphosphine. Selectivity for the monophosphine was attributed to the different reactivity of Zr–C(sp<sup>3</sup>) bonds between monoalkyl zirconocenes and zirconacyclopentadienes.

Transmetalation of Zr–C(sp<sup>2</sup>) to copper is a relatively recent development in organozirconium chemistry, and is proving to be a highly effective methodology for performing a range of carbon–carbon bond formation reactions with zirconacyclopentadienes. For instance, recent applications of copper-mediated or -catalyzed reactions of zirconacyclopentadienes include the stereoselective double allylation of zirconacyclopentadienes to afford stereodefined 1,4,6,9-tetraenes,<sup>16a</sup> the synthesis of fused aromatics via the coupling of zirconacyclopentadienes with dihaloaromatics,<sup>16b</sup> the highly selective one-pot formation of benzene derivatives by intermolecular coupling of three different alkynes,<sup>16c</sup> the formation of cyclopentenones via regioselective intermolecular coupling of trisubstituted alkenes, alkynes, and isocyanates,<sup>16d</sup> formation of fully substituted cyclooctatetraenes,<sup>16e,f</sup> the synthesis of vinylcyclohexadienes and methylenecycloheptadienes via tandem inter- and then intramolecular allylation of zirconacyclopentadienes,<sup>16g</sup> a new pathway to eight- and nine-membered-ring derivatives involving the copper-catalyzed intermolecular [4 + 4] and [4 + 5] coupling of zirconacyclopentadienes with bis(halomethyl)aromatics,<sup>16h</sup> the formation of cyclopentadiene derivatives and spirocyclic compounds by reaction of zirconacyclopentadienes with 1,1-dihalo compounds and enones,<sup>16i,j</sup> and the preparation of benzocycloheptene derivatives.<sup>16k</sup>

Surprisingly, the reductive coupling of 1-phenyl-1-propyne occurs with remarkable regioselectivity to give, after transmetalation and reaction with chlorodiphenylphosphine, the corresponding diphosphine 1,4-bis(diphenylphosphino)-1,3-diphenyl-2,4-dimethyl-1,3-butadiene (**2c**; 1,3-Ph<sub>2</sub>-2,4-Me<sub>2</sub>-NUPHOS).

Chart 1



The regioselectivity of this coupling was clearly apparent from the <sup>31</sup>P{<sup>1</sup>H} NMR spectrum of **2c**, which contains two singlets at δ –2.4 and –6.4 ppm of equal intensity and a pair of singlets at δ –3.4 and –2.3 (<5%), the latter of which most likely corresponds to minor amounts of the other two possible regioisomers (Chart 1). The <sup>1</sup>H spectrum of **2c** supports this assignment and contains a singlet at δ 2.02 and a doublet of doublets at δ 1.60 (*J*<sub>PH</sub> = 3.1 Hz, *J*<sub>PM</sub> = 1.3 Hz), which correspond to the methyl groups at the 4- and 2-positions of the butadiene tether, respectively. These methyl groups appear as a triplet at δ 25.1 (*J*<sub>PC</sub> = 8.1 Hz) and a doublet at δ 17.2 (*J*<sub>PC</sub> = 3.8 Hz) in the <sup>13</sup>C{<sup>1</sup>H} NMR spectrum. The alternative explanation, that the former resonances correspond to a 1:1 mixture of regioisomers **2c'** and **2c''** and that the minor signals belong to **2c**, was eliminated, since these latter signals clearly had vastly disparate intensities. Crystallization of the crude reaction product by slow diffusion of hexane into a toluene solution at room temperature gave **2c** as the sole product (isolated yield 66%), and the substitution pattern of the 1,3-diene tether was finally unequivocally established by a single-crystal X-ray structure determination of its palladium dichloride derivative (vide infra).

The intermolecular coupling of unsymmetrical internal alkynes has not been widely investigated as a synthetic methodology, since the factors that control the regiochemical outcome of this reaction are not well understood. The generation of Negishi's reagent in the presence of an unsymmetrical internal alkyne would be expected to give a statistical mixture of the three possible regioisomers. However, under certain circumstances the regioselectivity of coupling appears to be predictable, on the basis of the nature of the substituents. For example, coupling of the zirconocene complex of 1-hexyne with a 1-trimethylsilyl-substituted internal alkyne, such as 1-(trimethylsilyl)-1-propyne, gives a 1:1 mixture of regioisomers which after heating isomerize to give the metallacycle with the trimethylsilyl substituent in the α-position, as the sole product (Scheme 3).<sup>17</sup> Both electronic and steric factors were believed to be responsible for the regiochemical outcome of this reaction. The reductive coupling of phenylacetylene in the presence of Cp<sub>2</sub>Ti(PMe<sub>3</sub>)<sub>2</sub> has been reported to result in the selective formation of the α,α'-diphenyltitanacyclopentadiene, although no reasons were presented for the regiochemical outcome of this transformation.<sup>18</sup> On the basis of the above reports we might have expected the zirconium-mediated coupling of 1-phenyl-1-propyne to give the α,α'-diphenylzirconacyclopentadiene, since the

(14) Miyaji, T.; Xi, Z.; Nakajima, K.; Takahashi, T. *Organometallics* **2001**, 20, 2859.

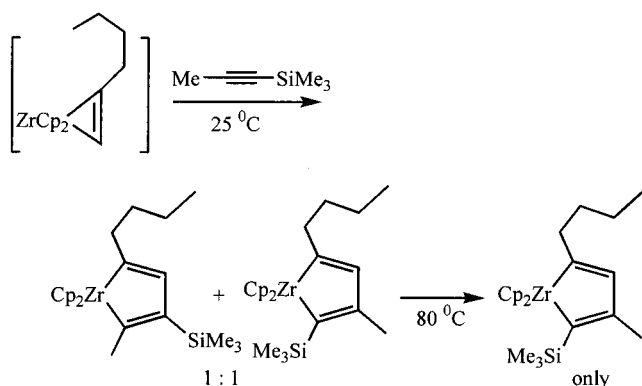
(15) (a) Nishihara, Y.; Aoyagi, K.; Hara, R.; Suzuki, N.; Takahashi, T. *Inorg. Chim. Acta* **1996**, 252, 91. (b) Aoyagi, K.; Kasai, K.; Kondakov, D. Y.; Hara, R.; Suzuki, N.; Takahashi, T. *Inorg. Chim. Acta* **1994**, 220, 319. (c) Mirza-Aghayan, M.; Boukherroub, O. G.; Manuel, G.; Koenig, M. J. *Organomet. Chem.* **1998**, 564, 61. (d) Mirza-Aghayan, M.; Boukherroub, O. G.; Etemad-Moghadam, G.; Manuel, G.; Koenig, M. *Tetrahedron Lett.* **1996**, 37, 3109.

(16) For a relevant review see: Takahashi, T.; Kotora, M.; Hara, R.; Xi, Z. *Bull. Chem. Soc. Jpn.* **1999**, 72, 2591. (a) Takahashi, T.; Kotora, M.; Kasai, K.; Suzuki, N.; Nakajima, K. *Organometallics* **1994**, 13, 4183. (b) Takahashi, T.; Hara, R.; Nishihara, Y.; Kotora, M. *J. Am. Chem. Soc.* **1996**, 118, 5154. (c) Takahashi, T.; Xi, Z.; Akiko, Y.; Liu, Y.; Nakajima, K.; Kotora, M. *J. Am. Chem. Soc.* **1998**, 120, 1672. (d) Takahashi, T.; Li, Y.; Tsai, F.-Y.; Nakajima, K. *Organometallics* **2001**, 20, 595. (e) Takahashi, T.; Sun, W.-H.; Nakajima, K. *Chem. Commun.* **1999**, 1595. (f) Yamamoto, Y.; Ohno, T.; Itoh, K. *Chem. Commun.* **1999**, 1543. (g) Kotora, M.; Umeda, C.; Ishida, T.; Takahashi, T. *Tetrahedron Lett.* **1997**, 38, 8355. (h) Takahashi, T.; Sun, W.-H.; Liu, Y.; Nakajima, K.; Kotora, M. *Organometallics* **1998**, 17, 3841. (i) Duan, Z.; Sun, W.-H.; Liu, Y.; Takahashi, T. *Tetrahedron Lett.* **2000**, 41, 7471. (j) Xi, C.; Kotora, M.; Nakajima, K.; Takahashi, T. *J. Org. Chem.* **2000**, 65, 945. (k) Takahashi, T.; Sun, W.-H.; Duan, Z.; Shen, B. *Org. Lett.* **2000**, 2, 1197.

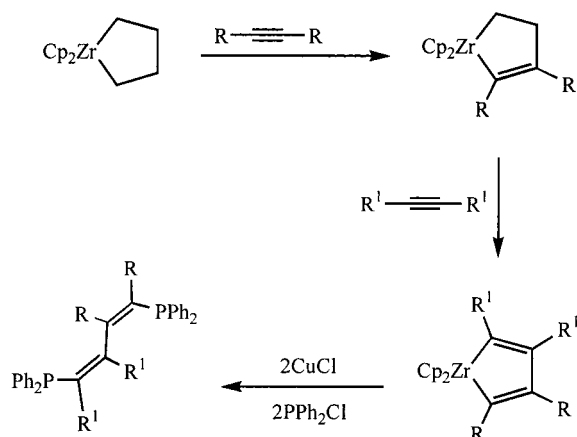
(17) Buchwald, S. L.; Neilsen, R. B. *J. Am. Chem. Soc.* **1989**, 111, 2870.

(18) Alt, H. G.; Engelhardt, H. E.; Rausch, M. D.; Kool, L. B. *J. Am. Chem. Soc.* **1985**, 107, 3717.

Scheme 3



Scheme 4

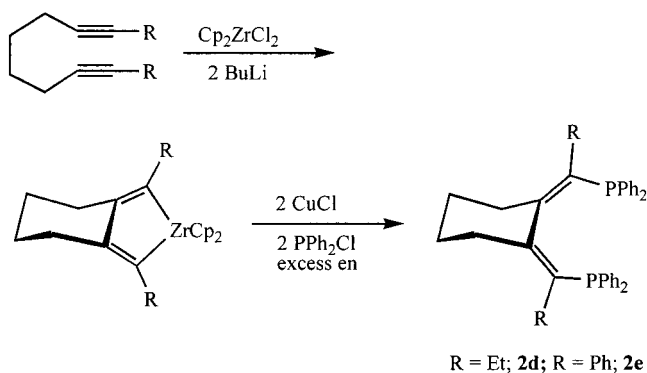


$\alpha$ -position is expected to be less hindered than the  $\beta$ -position. At this stage it is impossible to provide an explanation for the observed regioselectivity, and we cannot rule out initial formation of a mixture of regioisomers followed by equilibration to a single isomer.

While it will not be possible to prepare regioisomers **2c'** and **2c''** using this methodology, we note that it should be possible to prepare a variety of unsymmetrically substituted NUPHOS derivatives by exploiting the facile  $\text{C}_\beta\text{--C}_{\beta'}$  bond cleavage reaction of appropriately substituted zirconacyclopentenes<sup>19</sup> and zirconacyclopentadienes<sup>20</sup> in the presence of an alkyne to give the corresponding unsymmetrical zirconacyclopentadiene selectively, prior to quenching with chlorodiphenylphosphine, according to the procedure shown in Scheme 4.

To develop chiral versions of NUPHOS, it will be necessary to apply the methodology described above to chiral diynes. With this in mind, we have shown that 1,8-diphenyloctadiyne and 3,9-dodecadiyne undergo a reductive cyclization transmetalation sequence to afford the corresponding four-carbon-bridged diphosphines 1,2-bis(1-(diphenylphosphino)benzylidene)cyclohexane (**2d**; 1,4- $\text{Ph}_2$ -2,3-cyclo- $\text{C}_6\text{H}_8$ -NUPHOS) and 1,2-bis(1-(diphenylphosphino)prop-1-ylidene)cyclohexane (**2e**; 1,4- $\text{Et}_2$ -2,3-cyclo- $\text{C}_6\text{H}_8$ -NUPHOS), respectively (Scheme 5). We have successfully isolated a crystalline sample of

Scheme 5



the copper-coordinated diphosphine derived from 3,9-dodecadiyne by slow diffusion of methanol into a chloroform solution at room temperature, and a single-crystal X-ray study has been undertaken (vide infra). The  $^{31}\text{P}\{^1\text{H}\}$  spectra of **1d** and **1e** contain quadrupole-broadened resonances at  $\delta -3.0$  and  $-2.6$ , respectively, with a half-height line width ( $\Delta\nu_{1/2}$ ) similar to those of **1a–c**. Although the  $^{31}\text{P}$  NMR resonance of **1d** is broadened by quadrupolar effects ( $^{63}\text{Cu}$ ,  $I = 9/2$ ), the resonances in the  $^1\text{H}$  NMR spectrum are fairly narrow, since the line widths depend on the distance from the copper nucleus. The  $^1\text{H}$  NMR spectrum of **1d** contains a distinctive triplet at  $\delta 0.38$  ( $J = 7.6$  Hz) and a broad unresolved multiplet at  $\delta 1.25$  which correspond to the ethyl group attached to the diphenylphosphino carbon. The resonances associated with the methylene groups of the cyclohexane ring appear as four separate sets of signals between  $\delta 1.4$  and  $2.1$  ppm.

**X-ray Structure of Bis[chloro{1,2-bis(1-(diphenylphosphino)prop-1-ylidene)cyclohexane}copper] (1d) and 1,4-Bis(diphenylphosphino)-1,2,3,4-tetraphenyl-1,3-butadiene (2a).** As the synthetic methodology used to prepare **2a–e** involves the generation of an intermediate copper complex, we have undertaken a single-crystal X-ray structure determination of one of these, **1d**, to establish the mode of coordination and extent of aggregation. Single crystals of **1d**· $2\text{CHCl}_3$ · $2\text{MeOH}$  suitable for X-ray analysis were grown from a chloroform solution layered with methanol. A perspective view of the molecular structure of **1d** together with the atomic numbering scheme is shown in Figure 1; a selection of bond lengths and angles is listed in Table 1, and details of the crystal data are given in Table 8. The structure reveals that **1d** exists as a halide-bridged dimer, a feature common to many copper phosphine complexes, including  $[\text{Cu}(\text{PPh}_2\text{CH}_2\text{CH}(\text{OPPh}_2)\text{Cl})_2]$ , bis[chloro(*o*-phenylenebis(diisopropylphosphine))copper], and bis[bromo((2,3-dimethyl-2-silabut-3-enyl)diphenylphosphine)copper].<sup>21–23</sup> The copper atoms are bridged asymmetrically by the two chlorine atoms ( $\text{Cu}(1)\text{--Cl}(1) = 2.4564(6)$  Å,  $\text{Cu}(2)\text{--Cl}(1) = 2.3491(6)$  Å), with the difference in the Cu–Cl bond lengths of  $0.1073$  Å being similar to that recently reported for  $[\text{Cu}(\text{PPh}_2\text{CH}_2\text{CH}(\text{OPPh}_2)\text{Cl})_2]$ .<sup>21</sup> As expected, the coordination

(19) Takahashi, T.; Kegeyama, M.; Denisov, V.; Hara, R.; Negishi, E. *Tetrahedron Lett.* **1993**, 34, 687. (b) van Wagenen, B. C.; Livinghouse, T. *Tetrahedron Lett.* **1989**, 30, 3495. (c) Xi, Z.; Hara, R.; Takahashi, T. *J. Org. Chem.* **1995**, 60, 4444.

(20) Hara, R.; Xi, Z.; Kotora, M.; Xi, C.; Takahashi, T. *Chem. Lett.* **1996**, 1004.

(21) Bayler, A.; Schier, A.; Schmidbaur, H. *Inorg. Chem.* **1998**, 37, 4353.

(22) Baker, R. T.; Calabrese, J. C.; Westcott, S. A. *J. Organomet. Chem.* **1995**, 498, 109.

(23) Alyea, E. C.; Meehan, P. R.; Ferguson, G.; Kannan, S. *Polyhedron* **1997**, 16, 3479.

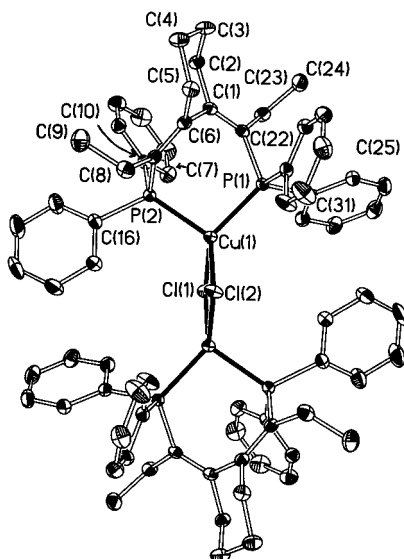


**Figure 1.** Molecular structure of  $[\text{CuCl}(1,4\text{-Et}_2\text{-}2,3\text{-cyclo-C}_6\text{H}_8\text{-NUPHOS})]_2$  (**1d**). Hydrogen atoms and  $\text{CHCl}_3$  and MeOH molecules of crystallization have been omitted for clarity. Ellipsoids are at the 50% probability level. Ring atoms are numbered sequentially in all structures.

**Table 1.** Selected Bond Distances (Å) and Angles (deg) for **1d**

Cu(1)–P(1)	2.2721(6)	Cu(1)–P(2)	2.2613(6)
Cu(1)–Cl(1)	2.4564(6)	Cu(1)–Cl(2)	2.3491(6)
P(1)–C(22)	1.846(2)	P(2)–C(7)	1.836(2)
C(22)–C(1)	1.347(3)	C(1)–C(6)	1.501(3)
C(6)–C(7)	1.349(3)		
P(1)–Cu(1)–P(2)	99.11(2)	Cl(1)–Cu(1)–Cl(2)	91.12(2)
P(1)–Cu(1)–Cl(1)	126.87(2)	P(1)–Cu(1)–Cl(2)	114.95(2)
P(2)–Cu(1)–Cl(1)	109.23(2)	P(2)–Cu(1)–Cl(2)	116.88(2)
C(6)–C(7)–P(2)	122.55(18)	C(8)–C(7)–P(2)	114.99(17)
C(8)–C(7)–C(6)	122.0(2)	C(1)–C(6)–C(5)	111.93(19)
C(5)–C(6)–C(7)	122.7(2)	C(1)–C(6)–C(7)	125.0(2)
C(2)–C(1)–C(22)	123.1(2)	C(2)–C(1)–C(6)	110.39(19)
C(6)–C(1)–C(22)	126.3(2)	C(23)–C(22)–C(1)	121.2(2)
C(23)–C(22)–P(1)	118.03(16)	C(3)–C(4)–C(5)	111.1(2)
C(4)–C(5)–C(6)	111.5(2)	C(2)–C(3)–C(4)	110.5(2)
C(1)–C(2)–C(3)	110.30(19)		

sphere around Cu(1) is close to tetrahedral with a dihedral angle of  $82.3^\circ$  between the planes containing P(1), Cu(1), P(2) and Cu(1), Cl(1), Cl(2). The Cu–P bond lengths of 2.2721(6) and 2.2613(6) Å for Cu(1)–P(1) and Cu(1)–P(2), respectively, are similar to those reported for copper complexes of bidentate diphosphines such as  $[\text{Cu}\{1,2\text{-bis(diphenylphosphino)ethylene}\}_2][\text{PF}_6]$  (2.276(2)–2.289(2) Å, mean 2.285(2) Å)<sup>24</sup> and  $[\text{Cu}(\text{dppf})\text{I}_2]$  (mean Cu–P distance 2.286(6) Å)<sup>25</sup> but significantly shorter than those in  $[\text{Cu}(\text{PPh}_3)_4][\text{PF}_6]$  (mean Cu–P distance of 2.54(6) Å).<sup>26</sup> The natural bite angle P(1)–Cu(1)–P(2) of  $99.11(2)^\circ$  is similar to that of  $98.98(3)^\circ$  in the recently reported  $[\text{Cu}\{(\text{S})\text{-BINAP}\}(\text{MeCN})_2][\text{ClO}_4]$ <sup>27</sup> and significantly larger than that of  $92.066(15)^\circ$  in the palladium NUPHOS derivative  $[(1,2,3,4\text{-Ph}_4\text{-NUPHOS})\text{PdCl}_2]$ , presumably due to its

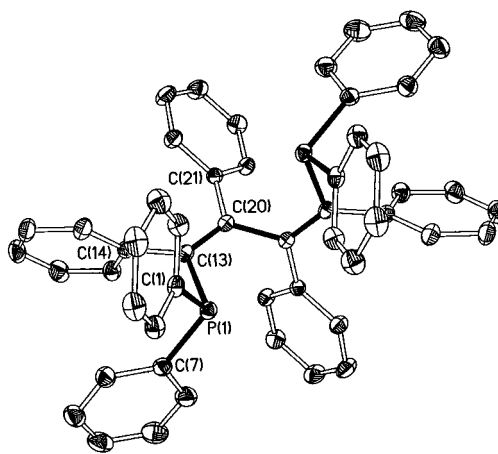


**Figure 2.** Molecular structure of 1,4-bis(diphenylphosphino)-1,2,3,4-tetraphenyl-1,3-butadiene (**2a**). Hydrogen atoms have been omitted for clarity. Ellipsoids are at the 40% probability level.

**Table 2.** Selected Bond Distances (Å) and Angles (deg) for **2a**

P(1)–C(7)	1.8265(13)	P(1)–C(13)	1.8436(12)
P(1)–C(1)	1.8334(13)	C(13)–C(20)	1.3505(16)
C(20)–C(20A)	1.518(2)	C(13)–C(14)	1.4954(16)
C(20)–C(21)	1.4933(16)		
C(7)–P(1)–C(1)	106.37(6)	C(1)–P(1)–C(13)	100.25(5)
C(7)–P(1)–C(13)	99.68(6)	C(20)–C(13)–P(1)	117.41(9)
C(20)–C(13)–C(14)	124.31(10)	C(14)–C(13)–P(1)	117.89(8)
C(21)–C(20)–C(20A)	114.17(10)	C(13)–C(20)–C(21)	124.07(10)
C(13)–C(20)–C(20A)	121.57(11)		

approximate tetrahedral geometry. The bonding in the four-carbon tether is highly localized; the C(1)–C(22) and C(6)–C(7) bond lengths of 1.347(3) and 1.349(3) Å, the planar nature of C(6), C(7), C(1), and C(22), and the dihedral angles of  $2.4$  and  $7.0^\circ$  between the pairs of planes C(6)C(5)C(1)/C(7)P(2)C(8) and C(1)C(6)C(2)/C(22)P(1)C(23), respectively, are consistent with  $\text{C}(\text{sp}^2)$ – $\text{C}(\text{sp}^2)$  double bonds, while the C(1)–C(6) bond length of 1.501(3) Å is close to that expected for a  $\text{C}(\text{sp}^2)$ – $\text{C}(\text{sp}^2)$  single bond. The C(1)–C(22) and C(6)–C(7) bond lengths (average 1.347 Å) are similar to the carbon–carbon double bond length of 1.337(12) Å, which bridges the two diphenylphosphino groups in  $[\text{Cu}\{1,2\text{-bis(diphenylphosphino)ethylene}\}_2][\text{PF}_6]$ .<sup>24</sup> The internal angles of the cyclohexane ring are all close to the expected value of  $109.5^\circ$ , including those of the exocyclic double bond, C(1) ( $\angle\text{C}(2)\text{C}(1)\text{C}(6) = 110.39(19)^\circ$ ) and C(6) ( $\angle\text{C}(1)\text{-C}(6)\text{C}(5) = 111.93(19)^\circ$ ), which are  $\text{sp}^2$ -hybridized. As a result, there is a marked deviation of the three interbond angles at C(6) and C(1) from the regular angle of  $120^\circ$ , presumably due to the angular constraints imposed by the chairlike six-membered ring.

A single-crystal X-ray analysis of diphosphine **2a** has also been carried out to establish precise details of the conformational arrangement of the 1,3-diene tether. Crystals of **2a** suitable for X-ray analysis were grown by slow diffusion of hexane into a toluene solution at room temperature. The molecular structure together with the atomic numbering scheme is shown in Figure 2, and a selection of bond lengths and angles is given in Table 2. The 1,3-diene skeleton is highly skewed toward the s-transoid conformation rather than s-cisoid with a torsion angle of  $113.3^\circ$  from the central single bond C(13)C(20)C(20A)C(13A). This angle is signifi-

(24) Berners-Price, S. J.; Colquhoun, L. A.; Healy, P. C.; Byriel, K. A.; Hanna, J. V. *J. Chem. Soc., Dalton Trans.* **1992**, 3357.

(25) Neo, S. P.; Zhou, Z.-Y.; Mak, T. C. W.; Hor, A. T. S. *J. Chem. Soc., Dalton Trans.* **1994**, 3451.

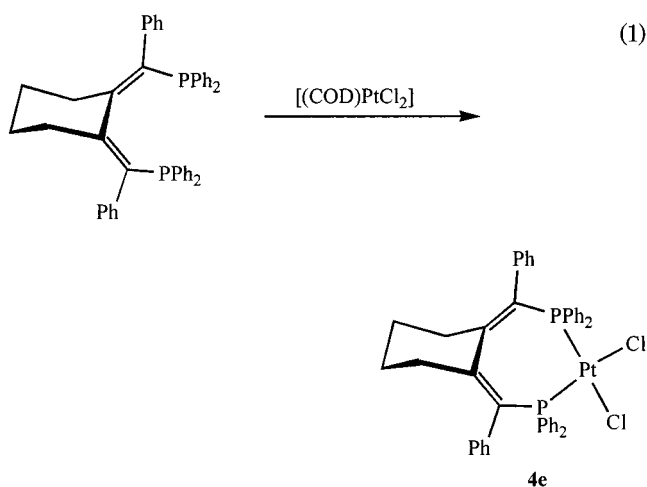
(26) Bowmaker, G. A.; Healy, P. C.; Engelhardt, L. M.; Kildea, J. D.; Skelton, B. W.; White, A. H. *Aust. J. Chem.* **1990**, *43*, 1697.

(27) Ferraris, D.; Young, B.; Cox, C.; Drury, W. J.; Dudding, T.; Lectka, T. *J. Org. Chem.* **1998**, *63*, 6090.



cantly larger than the corresponding angle of  $35.7^\circ$  in 1,1'-bis(3,3,4,4-tetrafluoro-2-(diphenylphosphino)cyclobutene).<sup>28</sup> The observed conformation reduces steric repulsions between the bulky diphenylphosphino groups and the phenyl rings as well as lone-pair-lone-pair repulsions, and **2a** is therefore not preorganized to coordinate, since the corresponding angle in [(1,2,3,4-Ph<sub>4</sub>-NUPHOS)PdCl<sub>2</sub>] is  $47.7^\circ$ , which requires a rotation of  $27.5^\circ$  about the central carbon-carbon bond of the butadiene tether. For comparison, the dihedral angle between the two naphthyl rings in free BINAP<sup>29</sup> is  $88.3^\circ$ , while the values typically found for chelating BINAP are  $65$ – $77^\circ$ . The bonding in the butadiene tether is highly localized, and the C(13)–C(20) bond length of  $1.3505(16)$  Å is in the region expected for a C(sp<sup>2</sup>)–C(sp<sup>2</sup>) double bond, similar to that reported for octa-phenyl[4]radialene<sup>30</sup> and the diphenylphosphino-substituted alkenes (*E*)-[Ph<sub>2</sub>P(Ph)C=C(H)Ph],<sup>31</sup> (*Z*)-[Ph<sub>2</sub>P(Ph)C=C(H)Ph],<sup>31</sup> [(Ph<sub>2</sub>P)<sub>2</sub>C=C(H)Me],<sup>32</sup> and (*Z*)-[Ph<sub>2</sub>P(H)C=C(H)PPh<sub>2</sub>],<sup>24</sup> while the C(20)–C(20A) bond length of  $1.518(2)$  Å is slightly longer than that of the  $1.48 \pm 0.01$  Å expected for a single bond between sp<sup>2</sup>-hybridized carbon atoms. Although the sums of the bond angles at C(13) and C(20) are  $359.61$  and  $359.81^\circ$ , respectively, close to the value expected for an sp<sup>2</sup>-hybridized carbon, the interbond angles deviate significantly from the regular sp<sup>2</sup> value of  $120^\circ$ . Similar distortions have been noted in diphenylphosphino-substituted alkenes, including those in (*E*)- and (*Z*)-[Ph<sub>2</sub>P(Ph)C=CHPh].<sup>31</sup>

**Synthesis and Characterization of Palladium and Platinum Complexes of **2a–e**.** Dropwise addition of a dichloromethane solution of **2a–e** into a dichloromethane solution of [(cycloocta-1,5-diene)PdCl<sub>2</sub>] resulted in a gradual color change from pale yellow to yellow-orange with the formation of [(NUPHOS)PdCl<sub>2</sub>] (**3a–e**) in yields of up to 73%. In a similar manner, the platinum dichloride complex of **2e**, [(1,4-Ph<sub>2</sub>-2,3-cyclo-C<sub>6</sub>H<sub>8</sub>-NUPHOS)PtCl<sub>2</sub>] (**4e**), was also prepared in near-quantitative yield (eq 1).



Complexes **3a–e** and **4e** have been characterized using standard spectroscopic and analytical methods

and, in the case of **3b,c** and **4e**, by single-crystal X-ray crystallography. For each of the compounds **3a–e**, the <sup>31</sup>P{<sup>1</sup>H} NMR spectrum contains a single sharp resonance shifted downfield relative to that of the uncoordinated diphosphine, while that of **4e** contains a singlet at  $\delta$  1.2 ppm flanked by platinum satellites with  $J_{\text{Pt-P}} = 3054$  Hz, in the region expected for phosphorus trans to chloride. In the <sup>1</sup>H NMR spectrum of **4e** four distinct sets of resonances between  $\delta$  1 and 2 ppm correspond to the axial and equatorial protons of the cyclohexane ring, while the low-field region contains numerous well-resolved multiplets and a distinctive exchange-broadened signal at  $\delta$  8.57. A single low-field exchange-broadened resonance is a feature common to the <sup>1</sup>H NMR spectra of compounds **3a–e**. Although seemingly uncomplicated, the presence of a broad low-field signal prompted us to undertake a variable-temperature <sup>1</sup>H NMR study of **4e**, the result of which is shown in Figure 3. As the temperature is lowered, the resonance at  $\delta$  8.57 ppm broadens, disappears into the baseline (243 K), and eventually reappears as two well-separated multiplets at 9.19 and 7.86 ppm (♦ in Figure 3), each corresponding to 2H. Within the same temperature range the resonance at  $\delta$  7.79 broadens and ultimately gives rise to two ill-defined triplets at  $\delta$  7.91 and 6.69 ppm (● in Figure 3), also of intensity 2H, while two triplets at  $\delta$  6.75 and 6.72 ppm (■ in Figure 3), each of intensity 4H, begin to broaden and decoalesce. Even at 203 K these last two signals are not resolved and appear as broad resonances. The remaining signals are temperature independent and appear as sharp well-resolved multiplets over the entire temperature range (▼ in Figure 3). Analysis of the COSY <sup>1</sup>H NMR spectrum at room temperature and 193 K has been used to identify and assign the aromatic protons. The intensity and pattern of resonances in the room-temperature <sup>1</sup>H NMR spectrum of **4e** is consistent with time-averaged C<sub>2</sub> symmetry with seven temperature-independent multiplets, each of intensity 2H, belonging to the protons of two static phenyl rings and the para phenyl signals of the PPh<sub>2</sub> groups and four temperature-dependent resonances, of total intensity 16H (4:4:4:4), which correspond to the protons of two pairs of freely rotating phenyl rings. On the basis of the multiplicity and intensity of the former resonances, in particular the two doublets at  $\delta$  6.21 and 5.94 ( $J = 7.4$  Hz), we are confident that these signals correspond to the phenyl rings attached to the four-carbon tether, while those that show temperature-dependent <sup>1</sup>H NMR behavior correspond to the axial and equatorial phenyl rings of the diphenylphosphino groups. The low-temperature <sup>1</sup>H NMR spectrum of **4e** is consistent with nonequivalent ortho and meta positions of the diphenylphosphino phenyl rings as a result of restricted rotation about the P–Ph bonds. As the temperature is raised, exchange occurs between the ortho protons associated with signals A and B to give X and between the meta protons C and D to give Y. Examination of the space-filling model of **4e** (Figure 4) reveals that it is the phenyl rings on the four-carbon tether that are likely to experience the greatest barrier to rotation, since these lie close and

(28) Rettig, S. J.; Trotter, J. *Can. J. Chem.* **1977**, *55*, 3065.

(29) Deeming, A. J.; Speel, D. M.; Stchedroff, M. *Organometallics* **1997**, *16*, 6004.

(30) (a) Iyoda, M.; Otani, H.; Oda, M. *J. Am. Chem. Soc.* **1986**, *108*, 5371. (b) Ottersen, T.; Jelinski, L. W.; Kiefer, E.; Seff, K. *Acta Crystallogr.* **1974**, *B30*, 960.

(31) Bookham, J. L.; Smithies, D. M.; Wright, A.; Thornton-Pett, M.; McFarlane, W. *J. Chem. Soc., Dalton Trans.* **1998**, 811.

(32) Bookham, J. L.; Conti, F.; McFarlane, C. E.; McFarlane, W.; Thornton-Pett, M. *J. Chem. Soc., Dalton Trans.* **1994**, 1791.

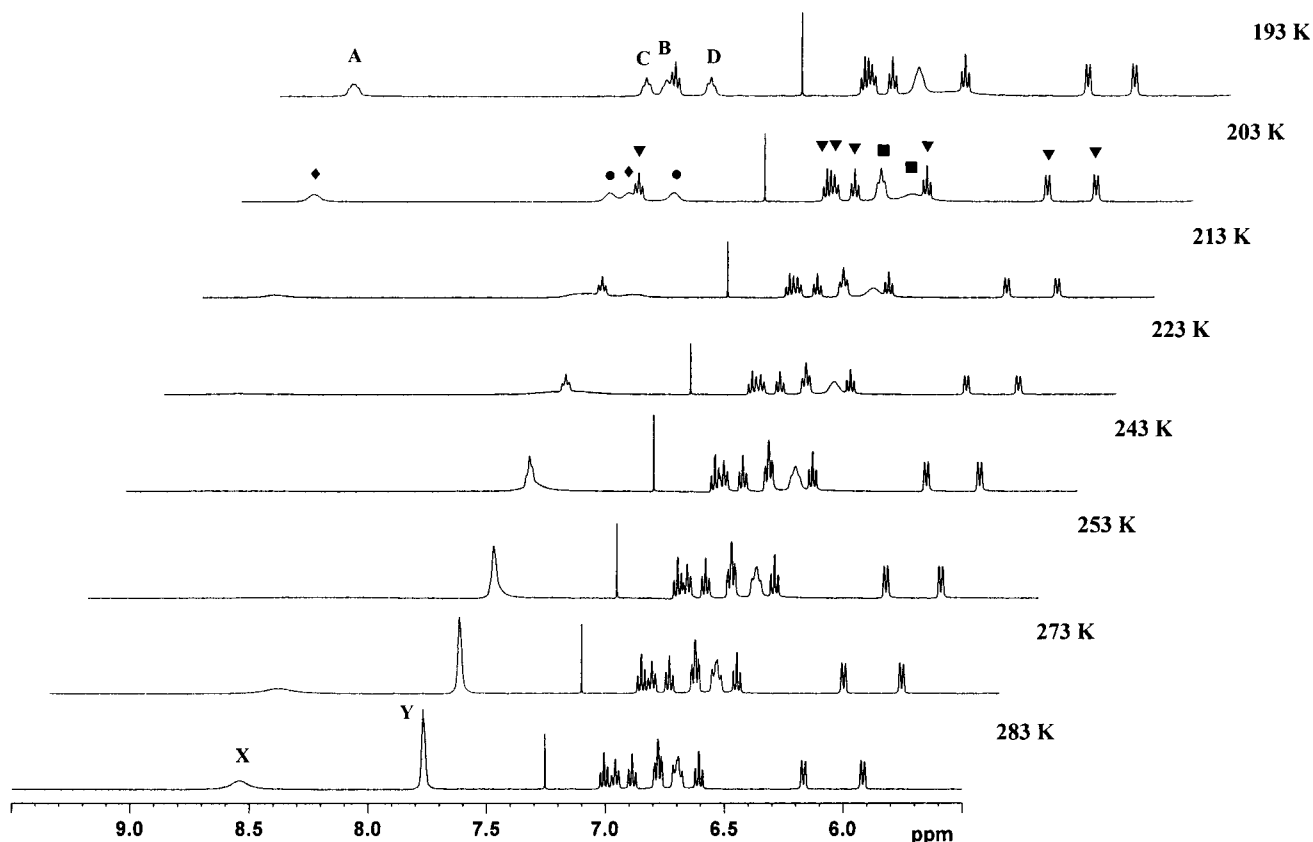


**Figure 3.** Variable-temperature  $^1\text{H}$  NMR spectra of  $[(1,4\text{-Ph}_2\text{-}2,3\text{-cyclo-C}_6\text{H}_8\text{-NUPHOS})\text{PtCl}_2]$  (**4e**) showing the pairwise coalescence of ortho phenyl signals and meta phenyl signals.

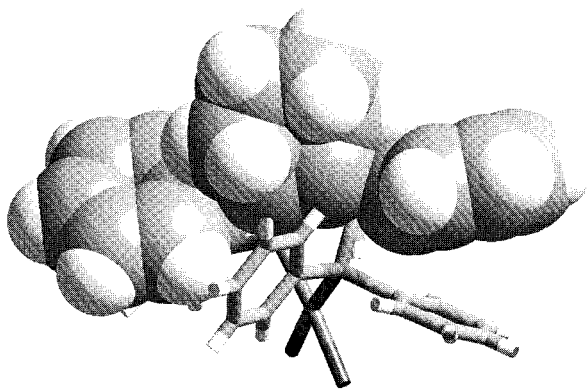


**Figure 4.** Space-filling model of **4e**. Rotation of the phenyl rings on the four-carbon tether is severely restricted, while the  $\text{PPh}_2$  phenyl rings experience a limited barrier to rotation.

parallel to the pseudoequatorial phenyl rings of the  $\text{PPh}_2$  group and are sandwiched between those rings and the equatorial hydrogen atom on the adjacent methylene group of the cyclohexyl ring. Variable-temperature  $^1\text{H}$  NMR studies have shown that this barrier must be sufficient to restrict rotation, even at room temperature on the NMR time scale. In contrast, the barrier to  $\text{P-Ph}$  rotation of the remaining four phenyl rings is significantly lower and can be monitored by  $^1\text{H}$  NMR spectroscopy. The barrier to rotation of the pseudoequatorial phenyl ring presumably arises from its close proximity to the phenyl ring on the four-carbon tether, while the barrier to rotation of its axial counterpart is most likely due to interactions between the

perpendicular oriented equatorial  $\text{P-Ph}$  and an axial hydrogen atom of the cyclohexyl ring. Restricted rotation about the  $\text{P-Ph}$  bonds of a coordinated BINAP has been reported, and it was assumed to be the pseudoaxial phenyl rings, since they lie close and parallel to the naphthyl groups and would thus experience the greatest barrier.<sup>29</sup> The temperature dependence of the  $^1\text{H}$  NMR spectra of **3a-e** bears a close similarity to that of **4e** in that the aromatic resonances of each, in particular those corresponding to the ortho protons, are strongly temperature dependent. In each case the chemical shift difference is ca. 1 ppm or greater, suggesting that the ortho sites are in very different environments in the temperature-limiting conformation.

**X-ray Structure of Dichloro[1,4-bis(diphenylphosphino)-1,2,3,4-tetramethyl-1,3-butadiene]platinum (3b), Dichloro[1,4-bis(diphenylphosphino)-1,3-dimethyl-2,4-diphenyl-1,3-butadiene]platinum (3c), and Dichloro[1,2-bis(diphenylphosphino)benzylidene]cyclohexane]platinum (4e).** The similarity between NUPHOS-type diphosphines and other biaryl-based phosphines such as BINAP and MeO-BIPHEP prompted us to undertake a single-crystal X-ray analysis of **3b**· $\text{CHCl}_3$  and **4e**· $4\text{CHCl}_3$  to provide precise details of the metal-ligand bonding and the conformation adopted by the chelate ring. Since there are three possible isomers of **2c** that would result from the nonselective intermolecular coupling of two unsymmetrical alkynes, a single-crystal X-ray structure determination of the palladium dichloride complex **3c**· $\text{CH}_2\text{Cl}_2$  was undertaken in order to unequivocally establish the regioselectivity of coupling. Perspective views of the molecular structures of **3b** and **3c** together



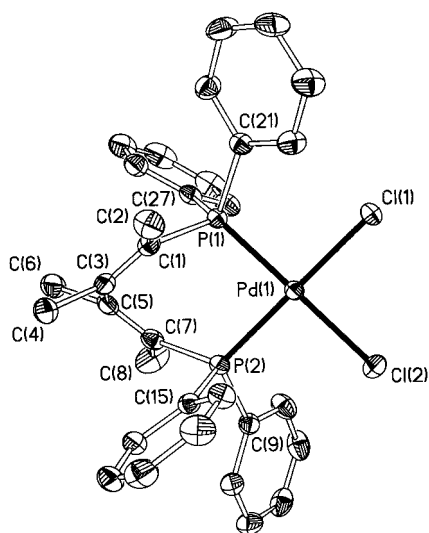


**Figure 5.** Molecular structure of [(1,2,3,4-Me<sub>4</sub>-NUPHOS)-PdCl<sub>2</sub>] (**3b**). Hydrogen atoms and the CHCl<sub>3</sub> molecule of crystallization have been omitted for clarity. Ellipsoids are at the 50% probability level.

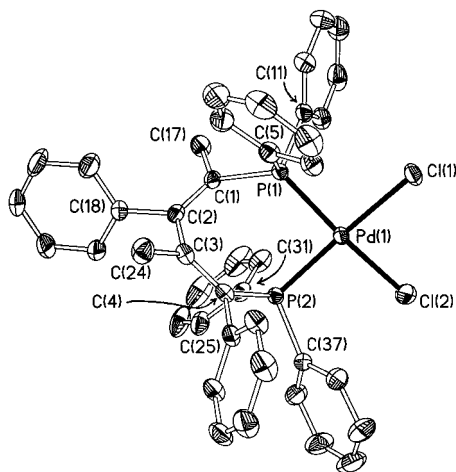


**Figure 6.** Molecular structure of [(1,3-Ph<sub>2</sub>-2,4-Me<sub>2</sub>-NUPHOS)-PdCl<sub>2</sub>] (**3c**). Hydrogen atoms and the CH<sub>2</sub>Cl<sub>2</sub> molecule of crystallization have been omitted for clarity. Ellipsoids are at the 50% probability level.

with their atomic numbering schemes are shown in Figures 5 and 6, respectively, and selected bond lengths and angles for both molecules are listed in Table 3. Since the structures of both compounds are based on palladium complexes of closely related four-carbon-bridged diphosphines, they will be discussed in parallel. The palladium atoms in **3b** and **3c** show a pronounced distortion from square planar, as indicated by the dihedral angles of 15.5 and 12.4°, respectively, between the planes containing P(1)P(2)Pd(1) and Pd(1)Cl(1)Cl(2) and marked deviations of the chlorides from the PdP<sub>2</sub> coordination plane (Cl(1) −0.5087 Å, Cl(2) 0.3669 Å for **3b** and Cl(1) 0.3618 Å, Cl(2) −0.3427 Å for **3c**). These distortions are comparable to those reported for [(BINAP)PdCl<sub>2</sub>],<sup>33</sup> [(BIPHEP)PdCl<sub>2</sub>],<sup>10</sup> and [(1,2,3,4-Ph<sub>4</sub>-NUPHOS)PdCl<sub>2</sub>],<sup>12</sup> all of which are based on structurally related four-carbon sp<sup>2</sup>-hybridized tethers. The natural bite angles of 89.817(18) and 90.37(3)° for **3b**

**Table 3.** Selected Bond Distances (Å) and Angles (deg) for **3b,c**

<b>3b</b>		<b>3c</b>	
Pd(1)–P(1)	2.2589(5)	Pd(1)–P(1)	2.2504(7)
Pd(1)–P(2)	2.2680(5)	Pd(1)–P(2)	2.2505(7)
Pd(1)–Cl(1)	2.3551(5)	Pd(1)–Cl(1)	2.3644(7)
Pd(1)–Cl(2)	2.3501(5)	Pd(1)–Cl(2)	2.3340(8)
P(1)–C(1)	1.8350(19)	P(1)–C(1)	1.842(3)
P(2)–C(7)	1.841(2)	P(2)–C(4)	1.849(3)
C(1)–C(3)	1.338(3)	C(1)–C(2)	1.343(4)
C(3)–C(5)	1.489(3)	C(2)–C(3)	1.502(4)
C(5)–C(7)	1.335(3)	C(3)–C(4)	1.352(4)
P(1)–Pd(1)–P(2)	89.817(18)	P(1)–Pd(1)–P(2)	90.37(3)
Cl(1)–Pd(1)–Cl(2)	89.651(19)	Cl(1)–Pd(1)–Cl(2)	88.76(3)
P(1)–Pd(1)–Cl(2)	170.999(19)	P(1)–Pd(1)–Cl(2)	171.04(3)
P(2)–Pd(1)–Cl(1)	167.424(19)	P(2)–Pd(1)–Cl(1)	171.20(3)
P(1)–Pd(1)–Cl(1)	91.751(18)	P(1)–Pd(1)–Cl(1)	89.59(3)
Pd(2)–Pd(1)–Cl(2)	90.747(18)	Pd(2)–Pd(1)–Cl(2)	92.61(3)
P(1)–C(1)–C(3)	122.11(15)	P(1)–C(1)–C(17)	116.38(19)
P(1)–C(1)–C(2)	115.20(14)	P(1)–C(1)–C(2)	121.6(2)
C(2)–C(1)–C(3)	122.34(18)	C(2)–C(1)–C(17)	122.0(2)
C(1)–C(3)–C(4)	123.0(2)	C(1)–C(2)–C(18)	120.1(2)
C(1)–C(3)–C(5)	123.29(18)	C(1)–C(2)–C(3)	125.2(2)
C(4)–C(3)–C(5)	113.70(18)	C(3)–C(2)–C(18)	114.4(2)
C(3)–C(5)–C(7)	122.30(18)	C(4)–C(3)–C(24)	121.5(3)
C(3)–C(5)–C(6)	114.63(18)	C(2)–C(3)–C(24)	114.0(2)
C(6)–C(5)–C(7)	122.9(2)	C(2)–C(3)–C(4)	124.5(2)
P(2)–C(7)–C(8)	116.40(16)	P(2)–C(4)–C(25)	115.12(19)
P(2)–C(7)–C(5)	121.76(15)	P(2)–C(4)–C(3)	124.1(2)
C(5)–C(7)–C(8)	121.82(19)	C(3)–C(4)–C(25)	120.6(2)

and **3c**, respectively, are close to the ideal value of 90° and are only slightly smaller than those in [(1,2,3,4-Ph<sub>4</sub>-NUPHOS)PdCl<sub>2</sub>] (92.066(15)°) and [(BIPHEP)PdCl<sub>2</sub>] (92.24(4)°). The remaining cis angles in **3b** (∠Cl(1)–Pd(1)Cl(2) = 89.651(19)°, ∠P(2)Pd(1)Cl(2) = 90.747(18)°, ∠P(1)Pd(1)Cl(1) = 91.751(18)°) and **3c** (∠Cl(1)Pd(1)–Cl(2) = 88.76(3)°, ∠P(2)Pd(1)Cl(2) = 92.61(3)°, ∠P(1)–Pd(1)Cl(1) = 89.59(3)°) are all close to the expected value of 90°. The corresponding trans angles in **3b** (∠P(2)–Pd(1)Cl(1) = 167.424(19)°, ∠P(1)Pd(1)Cl(2) = 170.999(19)°) and **3c** (∠P(2)Pd(1)Cl(1) = 171.20(3)°, ∠P(1)–Pd(1)P(2) = 171.04(3)°) are slightly smaller than is commonly found in related palladium complexes. Similar distortions away from square-planar geometry in [PdBr(*p*-NC-C<sub>6</sub>H<sub>4</sub>){(*S*)-MeO-BIPHEP}] have been described as a rotation of the P–Pd–P and Cl–Pd–Cl planes relative to one another, and not a tetrahedral distortion.<sup>34</sup> In comparison, the BINAP complex [PdBr(*p*-NC-C<sub>6</sub>H<sub>4</sub>){*p*-tol-BINAP}]<sup>34</sup> showed only minor distortions from a regular square-planar geometry. While the Pd–Cl bond lengths in **3b** are essentially the same (Pd(1)–Cl(1) = 2.3551(5) Å, Pd(1)–Cl(2) = 2.3501(5) Å) and are within the range reported for the structurally related complexes [(BINAP)PdCl<sub>2</sub>]<sup>33</sup> and [(BIPHEP)PdCl<sub>2</sub>],<sup>10</sup> those in **3c** are markedly disparate (Pd(1)–Cl(1) = 2.3644(7) Å, Pd(1)–Cl(2) = 2.3340(8) Å). In both complexes, the 1,3-butadiene bridged diphosphine coordinates to form a seven-membered chelate ring with a distorted-skew-boat conformation, in much the same manner as BINAP, BIPHEP, MeO-BIPHEP, and BIPHEMP. The dihedral angle of 63.0° between the least-squares plane containing the two sp<sup>2</sup> carbon atoms and their substituents C(1)C(2)C(3)C(4) and C(5)C(6)C(7)C(8) in **3b** is slightly larger than the corresponding

(33) Ozawa, F.; Kubo, A.; Matsumoto, Y.; Hayashi, T.; Nishioka, E.; Yanagi, K.; Moriguchi, K. *Organometallics* **1993**, *12*, 4188.

(34) (a) Drago, D.; Pregosin, P. S.; Tschoerner, M.; Albinati, A. *J. Chem. Soc., Dalton Trans.* **1999**, 2279. (b) Magistrato, A.; Merlin, M.; Pregosin, P. S.; Rothlisberger, U.; Albinati, A. *Organometallics* **2000**, *19*, 3591.

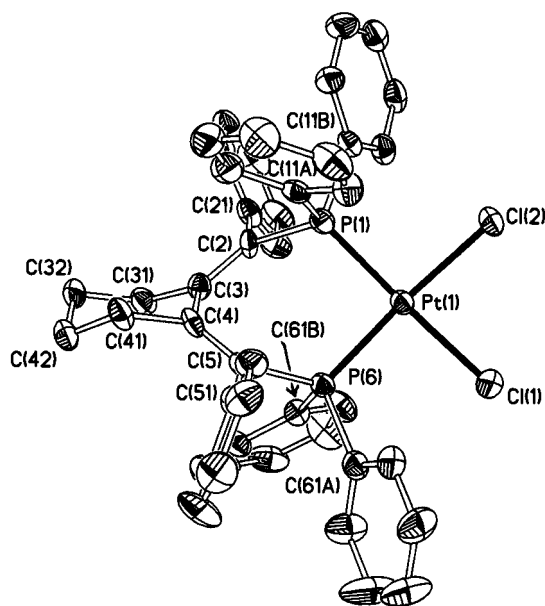


**Figure 7.** Molecular structure of [(1,4-Ph<sub>2</sub>-2,3-cyclo-C<sub>6</sub>H<sub>8</sub>-NUPHOS)PtCl<sub>2</sub>] (**4e**). Hydrogen atoms and CHCl<sub>3</sub> molecules of crystallization have been omitted for clarity. Ellipsoids are at the 50% probability level.

angle of 52.1° between C(3)C(4)C(24)C(25) and C(1)C(2)C(7)C(8) in **3c**. These angles are similar to that reported for [Rh{(R)-1,11-bis(diphenylphosphino)-5,7-dihydrodibenz[*c,e*]oxepin}(nbd)][BF<sub>4</sub>]<sup>3</sup> (55.9°) and [(1,2,3,4-Ph<sub>4</sub>-NUPHOS)PdCl<sub>2</sub>]<sup>12</sup> (47.7°). The pseudoaxial *P*-phenyl rings C(15)–C(20) and C(27)–C(32) of **3b** expose their edges toward the palladium atom to form torsional angles of 12.5 and 20.8°, respectively, while the spatial arrangement of the pseudoequatorial *P*-phenyl rings is intermediate between edge and face with torsional angles of 39.6 and 27.8° for the C(8)–C(14) and C(21)–C(26) rings, respectively. The *P*-phenyl rings in **3c** also adopt similar orientations with torsional angles of 21.1 and 9.0° for the pseudoaxial phenyl rings C(5)–C(10) and C(31)–C(36), respectively.

Unfortunately, we have been unable to grow crystals of the palladium complexes **3d,e** suitable for analysis by single-crystal X-ray crystallography. However, crystals of the platinum derivative of **2e**, dichloro[1,2-bis(diphenylphosphinobenzylidene)cyclohexane]platinum (**4e**), have been obtained from a saturated chloroform solution at room temperature. A perspective view of the molecular structure of **4e** together with the atomic numbering scheme is shown in Figure 7, and a selection of bond lengths and angles is listed in Table 4. Details of the crystal data are given in Table 8. The molecular structure shows that the coordination sphere around Pt(1) is close to square planar with a dihedral angle of 5.7° between the PtP<sub>2</sub> and PtCl<sub>2</sub> planes and deviations of –0.1123 and 0.1969 Å for Cl(1) and Cl(2), respectively, out of the PtP<sub>2</sub> coordination plane. The Pt(1)–P(1) and Pt(1)–P(6) bond lengths of 2.2453(18) and 2.2508(17) Å are within the range reported for platinum diphosphine complexes such as [Pt(BIPHEP)(BINOL)]<sup>35</sup> (average Pt–P distance = 2.2443(18) Å), as are the Pt–Cl bond lengths of 2.3507(18) and 2.3585(16) Å for Pt(1)–Cl(1) and Pt(1)–Cl(2), respectively. The natural bite angle of 92.25(6)° is comparable to those reported for [Pt(BIPHEP)(BINOL)]<sup>35</sup> (93.03(7)°), [Pt(BINAP)<sub>2</sub>]<sup>36</sup>

**Table 4.** Selected Bond Distances (Å) and Angles (deg) for **4e**

Pt(1)–P(1)	2.2453(18)	Pt(1)–P(6)	2.2508(17)
Pt(1)–Cl(1)	2.3507(18)	Pt(1)–Cl(2)	2.3585(16)
P(1)–C(2)	1.843(6)	P(6)–C(5)	1.860(7)
C(2)–C(3)	1.352(8)	C(3)–C(4)	1.501(9)
C(4)–C(5)	1.355(9)		
P(1)–Pt(1)–P(6)	92.25(6)	Cl(1)–Pt(1)–Cl(2)	85.88(6)
P(1)–Pt(1)–Cl(1)	176.02(6)	P(6)–Pt(1)–Cl(1)	90.64(6)
P(1)–Pt(1)–Cl(2)	91.47(6)	P(6)–Pt(1)–Cl(2)	173.93(6)
P(1)–C(2)–C(21)	114.3(2)	P(1)–C(2)–C(3)	125.8(5)
C(3)–C(2)–C(21)	119.9(6)	C(2)–C(3)–C(31)	123.1(6)
C(2)–C(3)–C(4)	123.5(6)	C(31)–C(3)–C(4)	113.3(5)
C(3)–C(4)–C(5)	124.7(6)	C(3)–C(4)–C(41)	113.7(6)
C(5)–C(4)–C(41)	121.5(6)	P(6)–C(5)–C(51)	116.0(5)
C(4)–C(5)–C(51)	120.9(6)	C(4)–C(5)–P(6)	123.1(5)
C(4)–C(41)–C(42)	109.8(6)	C(41)–C(42)–C(32)	110.2(5)
C(42)–C(32)–C(31)	111.6(6)	C(32)–C(31)–C(3)	112.1(6)

(92.3(1)°), [Pt{(R)-Tol-BINAP}(stilbene)]<sup>37</sup> (94.41(3)°), and [Pt{(R)-BINAP}(*o*-C<sub>6</sub>H<sub>5</sub>OMe)<sub>2</sub>] (93.1°)<sup>38</sup> and is characteristic of diphosphines bridged by four-carbon-atom sp<sup>2</sup>-hybridized tethers. The bonding in the 1,3-diene tether is highly localized with C(2)–C(3) and C(4)–C(5) bond lengths of 1.352(8) and 1.355(9) Å, respectively, close to that expected for a C(sp<sup>2</sup>)–C(sp<sup>2</sup>) double bond, and the C(3)–C(4) bond length of 1.501(9) Å is typical of a single bond between sp<sup>2</sup>-hybridized carbon atoms. There is a marked deviation of the interbond angles at C(3) and C(4) from the expected angle of 120° for an sp<sup>2</sup>-hybridized carbon. The angles of 113.3(5) and 113.7(6)° for C(4)C(3)C(31) and C(3)C(4)–C(41), respectively, reflect a strong tendency for these carbon atoms to adopt an angle close to 109.5°, required by a cyclohexane ring. To compensate, the remaining angles at C(3) and C(4) are much greater than the ideal value of 120°. In contrast to the structures of **3b** and **3c**, in which the NUPHOS ligand is highly distorted above the PdP<sub>2</sub> plane, that of **4e** is close to C<sub>2</sub> symmetry and the conformation of the four-carbon tether bears a close resemblance to that of many BINAP and BIPHEP derivatives. The dihedral angle between the least-squares planes containing C(4)C(41)C(5)C(51) and C(2)C(21)C(3)C(31) which defines the atropisomerism of NUPHOS is 53.3° and is similar to that in **3c**. The four rings of the diphenylphosphino groups are arranged in an alternating edge/face manner, as is often observed for atropisomeric diphosphines.<sup>39</sup> The two pseudoaxial phenyl rings expose their edges toward Pt(1) and form torsional angles of 27.5 and 34.7° for the C(61B) and C(11A) rings, and the pseudoequatorial rings expose their faces toward platinum to form torsional angles of 48.0 and 44.7° for C(61A) and C(11B), respectively.

**Kumada Coupling Reactions of Bromobenzene and 2-Bromopropene.** Hayashi and co-workers have recently reported the first use of dpbp (BIPHEP) for the

(35) Tudor, M. D.; Becker, J. J.; White, P. S.; Gagne, M. R. *Organometallics* **2000**, *19*, 4376.

(36) Tominaga, H.; Sakai, K.; Tsubomura, T. *J. Chem. Soc., Chem. Commun.* **1995**, 2273.

(37) Wicht, D. K.; Zhuravel, M. A.; Gregush, R. V.; Glueck, D. S.; Guzei, I. A.; Liabre-Sands, L. M.; Rheingold, A. L. *Organometallics* **1998**, *17*, 1412.

(38) (a) Alcock, N. W.; Brown, J. M.; Perez-Torrente, J. *Tetrahedron Lett.* **1992**, *33*, 389. (b) Brown, J. M.; Perez-Torrente, J. J.; Alcock, N. W. *Organometallics* **1995**, *14*, 1195.

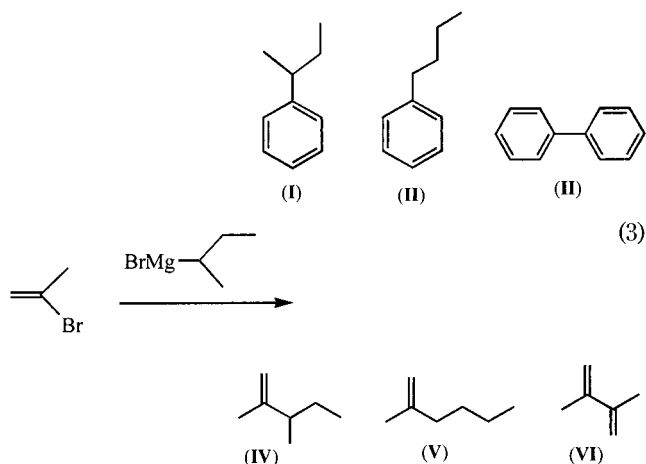
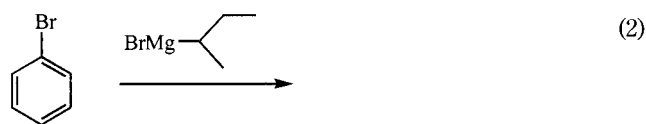
(39) Toriumi, K.; Ito, T.; Takaya, H.; Souchi, T.; Noyori, R. *Acta Crystallogr.* **1982**, *B38*, 807.

**Table 5. Cross-Coupling Reactions of Bromobenzene with *sec*-Butylmagnesium Chloride<sup>a</sup>**

entry	diphosphine	TOF <sup>b</sup>	GC yield (%) <sup>c</sup>
1	<b>2a</b>	6900	100 (3)
2	<b>2b</b>	270	78 (17)
3	<b>2c</b>	880	
4	<b>2d</b>	295	
5	<b>2e</b>	450	
6	BINAP	260	100 (22)
7	dppf	145	64 (22)

<sup>a</sup> Reaction conditions: 1.0 equiv of bromobenzene; 2 equiv of *sec*-butylmagnesium chloride (2.0 mol dm<sup>-3</sup>); 0.1 mol % [(diphosphine)PdCl<sub>2</sub>]; 0.5 equiv of *n*-decane internal standard; diethyl ether 1 mL/5 mmol bromide; substrate (R-Br) bromobenzene; amount of catalyst 0.1 mol %. <sup>b</sup> Initial turnover frequency in units of (mol of product) (mol of cat.)<sup>-1</sup> h<sup>-1</sup>, determined by GC analysis of the reaction mixture after hydrolysis with 10% HCl, based on consumption of starting material. <sup>c</sup> Determined by GC analysis of the reaction mixture, based on product. The reaction time (h) is given in parentheses.

palladium-catalyzed coupling of aryl and alkenyl bromides with *sec*-butylmagnesium bromide and the rhodium-catalyzed conjugate addition of phenyl boronic acids to enones.<sup>10</sup> In particular, they showed that the activity and selectivity of catalysts based on BIPHEP compare favorably with those formed from BINAP and dppf. Since the four-carbon tether of NUPHOS-type phosphines resembles that of BIPHEP and BINAP, we have examined the efficiency of these new diphosphines in the palladium-catalyzed cross-coupling of bromobenzene and 2-bromopropene (eqs 2 and 3). The coupling of



bromobenzene, to give *sec*-butylbenzene (**I**), is commonly used as a model reaction to compare catalyst activity and selectivity; the possible byproducts of this reaction being *n*-butylbenzene (**II**) and biphenyl (**III**) (eq 2). The results of catalyst testing of bromobenzene and 2-bromopropene are summarized in Tables 5 and 6, respectively. In all cases, catalysts formed from NUPHOS derivatives **2a–e** either rival or are far superior to those based on BINAP and dppf. Initial studies showed that [(1,2,3,4-Ph<sub>4</sub>-NUPHOS)PdCl<sub>2</sub>] catalyzes the cross-coupling of bromobenzene to give *sec*-butylbenzene at a

catalyst loading of 0.1 mol % Pd. The reaction mixture begins to reflux vigorously within minutes of adding the catalyst, and reaction is complete after only 30 min, resulting in an initial TOF of 6900 (mol of product) (mol of palladium)<sup>-1</sup> h<sup>-1</sup>. In contrast, under similar conditions catalysts formed from dppf and BINAP are significantly less active and require 5–7 h to reach completion, with initial TOF values of 145 and 260 (mol of product) (mol of palladium)<sup>-1</sup> h<sup>-1</sup>, respectively. The initial TOF of 6900 (mol of product) (mol of palladium)<sup>-1</sup> h<sup>-1</sup> achieved with 1,2,3,4-Ph<sub>4</sub>-NUPHOS is over 30 times greater than that of its dppf counterpart, which clearly demonstrates the impressive performance of NUPHOS-type diphosphines in palladium-catalyzed cross-couplings.

In one of the first studies of the influence of the diphosphine on the efficiency of palladium-catalyzed cross-couplings, Hayashi showed that [(dppf)PdCl<sub>2</sub>] catalyzes the reaction of bromobenzene with *sec*-butylmagnesium bromide to give *sec*-butylbenzene in near-quantitative yield (95%), while other phosphine-based palladium and nickel complexes were much less active, and in a number of cases less selective, generating significant quantities of *n*-butylbenzene byproduct.<sup>40</sup> In a recent and systematic examination of the effect of the bite angle of the diphosphine ( $\beta_n$ )<sup>41</sup> on the activity and selectivity of the palladium-catalyzed cross-coupling of bromobenzene, Kamer has shown that both selectivity and activity reach a maximum when the natural bite angle is ca. 100°. <sup>42</sup> In a comparative study of a range of Xantphos<sup>43</sup> type diphosphines, catalysts based on DPEphos ( $\beta_n = 102.7^\circ$ ) were found to be more active and selective than their dppf counterparts, with initial TOF values of 181 and 79 (mol of product) (mol of palladium)<sup>-1</sup> h<sup>-1</sup>, respectively.<sup>42b</sup> The dppf-based catalyst also generated small amounts of biphenyl byproduct (~ 3%), not reported in the early studies of Hayashi, whereas that based on DPEphos formed ca. 1% each of biphenyl and *n*-butylbenzene. An increase in the natural bite angle above 102.7° resulted in a significant reduction in activity and selectivity, with the amount of biphenyl reaching a maximum of 40% for Sixantphos ( $\beta_n = 110^\circ$ ). The high activity of dppf- and DPEphos-based catalysts has been attributed to the large natural bite angles of 99.07 and 102.7°, respectively, which forces the R–Pd–R angle in the diorgano intermediate to decrease, which effects an increase in the rate of reductive elimination. Diphosphines with bite angles greater than that of DPEphos result in a distortion toward tetrahedral coordination, which increases the R–Pd–R angle and results in a decrease in the rate of reductive elimination.

The activity of catalysts formed from NUPHOS type diphosphines **2a–e** show a dramatic dependence on the substituents attached to the 1,3-butadiene tether. For instance, substitution of the phenyl groups for methyl

(40) (a) Hayashi, T.; Konishi, M.; Kumada, M.; *Tetrahedron Lett.* **1979**, 21, 1871. (b) Hayashi, T.; Konishi, M.; Kobori, Y.; Kumada, M.; Higuchi, T.; Hirotsu, K. *J. Am. Chem. Soc.* **1984**, 106, 158.

(41) Casey, C. P.; Whiteker, G. T. *Isr. J. Chem.* **1990**, 20, 299.

(42) (a) van Leeuwen, P. W. N. M.; Kamer, P. C. J.; Reek, J. N. H.; Dierkes, P. *Chem. Rev.* **2000**, 100, 2741. (b) Kranenburg, M.; Kamer, P. C. J.; van Leeuwen, P. W. N. M. *Eur. J. Inorg. Chem.* **1998**, 155.

(43) Kranenburg, M.; van der Burgt, Y. E. M.; Kamer, P. C. J.; van Leeuwen, P. W. N. M.; Goubitz, K.; Fraanje, J. *Organometallics* **1995**, 14, 3081.



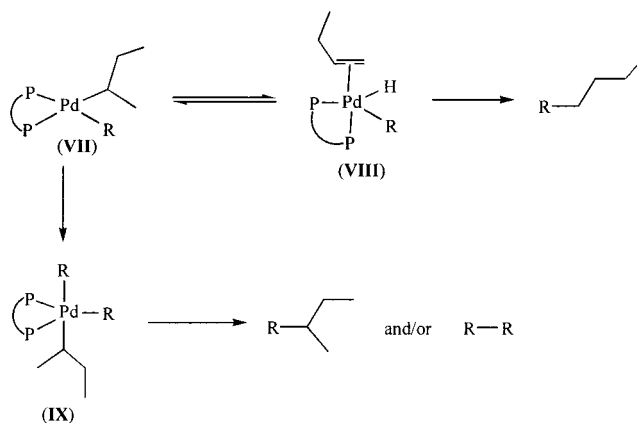
**Table 6.** Cross-Coupling Reaction of 2-Bromopropene with *sec*-Butylmagnesium Chloride<sup>a</sup>

Entry	Substrate	Diphosphine	Catalyst (mol%)	TOF <sup>b</sup>	2,3-dimethylpentene	2-methylhexene	2,3-dimethylbutadiene
1	2-bromopropene	<b>2a</b>	0.1	2200	98	1	< 1
2	2-bromopropene	<b>2b</b>	0.1	620	92	7	< 1
3	2-bromopropene	<b>2c</b>	0.1	2900	95	2	3
4	2-bromopropene	<b>2d</b>	0.1	1580	53	26	21
5	2-bromopropene	<b>2e</b>	0.1	951	37	29	34
6	2-bromopropene	<b>BINAP</b>	0.1	220	94	6	-
7	2-bromopropene	<b>dppf</b>	0.1	2200	99	-	-

<sup>a</sup> Reaction conditions: 1.0 equiv of 2-bromopropene; 2 equiv of *sec*-butylmagnesium chloride ( $2.0 \text{ mol dm}^{-3}$ ); 0.1 mol % [(diphosphine)-PdCl<sub>2</sub>]; 0.5 equiv of *n*-decane internal standard, diethyl ether 1 mL/5 mmol bromide. <sup>b</sup> Initial turnover frequency in units of (mol of product) (mol of cat.)<sup>-1</sup> h<sup>-1</sup>, determined by GC analysis of the reaction mixture after hydrolysis with 10% HCl, based on consumption of starting material.

groups results in a dramatic decrease in activity from 6900 to 880 and 270 (mol of product) (mol of cat.)<sup>-1</sup> h<sup>-1</sup> for [(1,3-Ph<sub>2</sub>-2,4-Me<sub>2</sub>-NUPHOS)PdCl<sub>2</sub>] and [(1,2,3,4-Me<sub>4</sub>-NUPHOS)PdCl<sub>2</sub>], respectively. Since the reductive coupling of 1-phenyl-1-propyne occurs selectively to give the 1,3-Ph<sub>2</sub>-2,4-Me<sub>2</sub> regioisomer as the sole product, it will be impossible to examine the performance of the other two regioisomers with 1,4-Me<sub>2</sub>-2,3-Ph<sub>2</sub> and 1,4-Ph<sub>2</sub>-2,3-Me<sub>2</sub> substitution. However, because of the geometrical constraints associated with intramolecular reductive coupling, the use of diynes to prepare NUPHOS derivatives incorporates the tether as part of a carbocycle and provides a means of selectively varying the substituents at the 1- and 4-positions. In the case of **2d,e**, the C<sub>4</sub> tether is comprised of two adjacent exocyclic double bonds of a cyclohexane ring and the 1,4-substituents are Et and Ph, respectively. Catalysts formed using ligands **2d,e** were found to be markedly less active than that of **2a** but comparable to those based on **2b,c**.

Isomerization<sup>40</sup> and homocoupling<sup>44</sup> are often major problems associated with cross-couplings involving secondary Grignard reagents, which in the case of *sec*-butylmagnesium bromide results in the formation of *n*-butylated byproduct, via a  $\beta$ -hydride elimination pathway and biphenyl, respectively. Kamer has suggested that the formation of *n*-butylbenzene results from an increasing tendency for large natural bite angle phosphines to stabilize the trigonal-bipyramidal hydrido-alkene intermediate (VIII), which increases the rate of  $\beta$ -hydride elimination compared to reductive elimination from [(diphos)Pd(R)(2-Bu)] (VII) (Scheme 6). Catalysts based on diphosphines **2a–e** are highly selective for cross-coupling *sec*-butylmagnesium bromide with bromobenzene and give exclusively the *sec*-butylated (I) product with no evidence for the formation of its *n*-butylated isomer (II) or biphenyl (III). Since the studies of Kamer involved Xantphos type diphosphines, all of which have similar steric and electronic properties, any effect on selectivity and activity was attributed to the bite angle. In contrast, the natural bite angles of NUPHOS type diphosphines are considerably smaller,

**Scheme 6**

all are typically close to 90°, and yet they all form catalysts that are considerably more efficient for the cross-coupling of bromobenzene. In fact, the bite angles of **2a–e** are similar to that of dppp, which has been shown to form catalysts with low *n/iso* selectivity and particularly poor activity. The impressive activity of NUPHOS-based catalysts and the pronounced influence of the nature of the four-carbon tether on catalyst performance requires further investigation in order to fully understand the origin of these effects. Although the reasons for the high activity of NUPHOS-based catalysts are not well understood, it is clear that bite angle effects alone are not responsible for the observed trends in activity and selectivity and the efficiency of catalysts based on **2a–e** is more likely to be due to a combination of factors.

In stark contrast to the high efficiency of catalysts based on NUPHOS-type diphosphines for the cross-coupling of bromobenzene, the performance of the same catalysts for coupling 2-bromopropene is highly dependent on the nature of the 1,3-diene tether. Specifically, catalysts based on the acyclic NUPHOS derivatives **2a–c** couple 2-bromopropane and *sec*-butylmagnesium bromide to give 2,3-dimethyl-1-pentene (IV) with high selectivity (92–98%) and with the formation of only minor amounts of the isomerization (V) and homocoupled (VI) byproducts 2-methyl-1-hexene and 2,3-

(44) van Asselt, R.; Elsevier, C. J. *Organometallics* **1994**, 13, 1972.

Table 7. Suzuki Cross-Coupling Reactions with Aryl Bromides<sup>a</sup>

entry	substrate (R–Br)	diphosphine	amt of cat. (mol %)	TOF <sup>b</sup>	GC yield %	approx time	TON
1	bromobenzene	<b>2a</b>	0.1	2250	75	20 min	750
2	bromobenzene	<b>2b</b>	0.1	1509	50	20 min	503
3	bromobenzene	<b>2c</b>	0.1	1230	41	20 min	410
4	bromobenzene	<b>2d</b>	0.1	1893	63	20 min	631
5	bromobenzene	<b>2e</b>	0.1	1458	49	20 min	486
6	bromobenzene	BINAP	0.1	2100	70	20 min	700
7	bromobenzene	dppf	0.1	1800	60	20 min	600
8	4-bromoacetophenone	<b>2a</b>	0.06	8700	87	10 min	1450
9	4-bromoacetophenone	<b>2b</b>	0.06	8300	83	10 min	1383
10	4-bromoacetophenone	<b>2c</b>	0.06	7600	76	10 min	1267
11	4-bromoacetophenone	<b>2d</b>	0.06	7900	79	10 min	1317
12	4-bromoacetophenone	<b>2e</b>	0.06	8500	85	10 min	1417
13	4-bromoacetophenone	BINAP	0.06	8600	86	10 min	1433
14	4-bromoacetophenone	dppf	0.06	8900	89	10 min	1483
15	4-bromoacetophenone	<b>2a</b>	0.0001		100	22 h	1000000
16	4-bromoacetophenone	<b>2b</b>	0.0001		82	43 h	820000
17	4-bromoacetophenone	<b>2c</b>	0.0001		90	20 h	900000
18	4-bromoacetophenone	<b>2d</b>	0.0001		99	20 h	990000
19	4-bromoacetophenone	<b>2e</b>	0.0001		100	20 h	1000000
20	4-bromoacetophenone	BINAP	0.0001		99	20 h	990000
21	4-bromoacetophenone	dppf	0.0001		100	21 h	1000000

<sup>a</sup> Reaction conditions: 1.0 equiv of aryl bromide; 1.5 equiv of phenylboronic acid; 2 equiv of K<sub>2</sub>CO<sub>3</sub>; diphosphine: Pd<sub>2</sub>(dba)<sub>3</sub> 1:2; DME (3 mL/mmol of aryl bromide); 0.43 equiv of *n*-decane internal standard; 85 °C. Reaction times have not been minimized. <sup>b</sup> Initial turnover frequency in units of (mol of product) (mol of cat.)<sup>−1</sup> h<sup>−1</sup>, determined by GC analysis of the reaction mixture after diluting with diethyl ether and filtration through Celite, based on consumption of starting material.

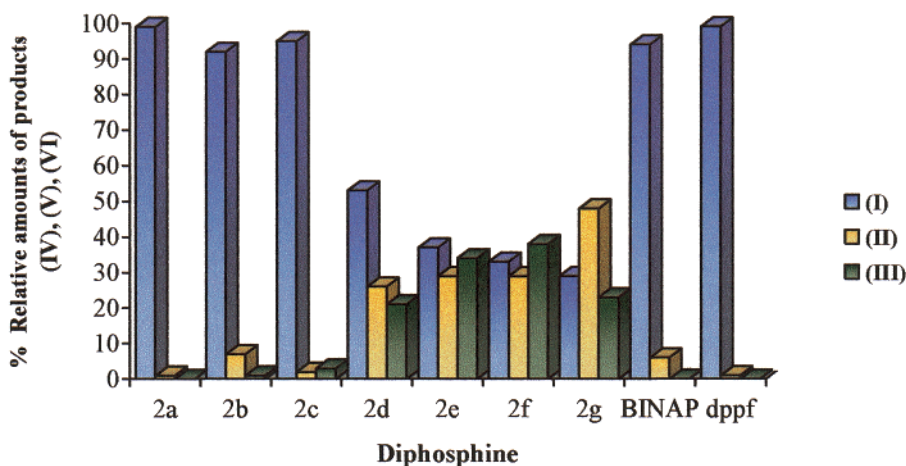


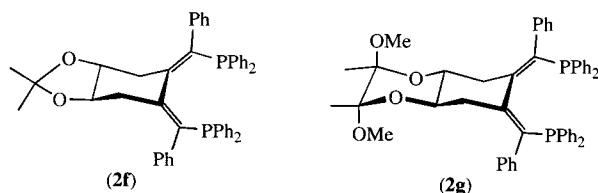
**Figure 8.** Graphical representation of the Grignard cross-coupling reaction between 2-bromopropene and *sec*-butylmagnesium bromide, illustrating the dramatic difference in selectivity for 2,3-dimethylpentene (I), 2-methylhexene (II), and 2,3-dimethylbutadiene (III) between catalysts based on **2a–c** and **2d–f**.

dimethylbutadiene, respectively (eq 3). The initial TOF values of 2200 and 2900 (mol of product) (mol of cat.)<sup>−1</sup> h<sup>−1</sup> for catalysts formed from **2a** and **2c**, respectively, are substantially higher than that of 800 (mol of product) (mol of cat.)<sup>−1</sup> h<sup>−1</sup> for **2b** and comparable to that of 2200 (mol of product) (mol of cat.)<sup>−1</sup> h<sup>−1</sup> obtained for [(dppf)PdCl<sub>2</sub>]. The high activity obtained using [(dppf)PdCl<sub>2</sub>] was somewhat unexpected, considering its poor performance in the cross-coupling of bromobenzene, for which a maximum TOF of 145 (mol of product) (mol of cat.)<sup>−1</sup> h<sup>−1</sup> was obtained. Under the same conditions the initial TOF of catalysts based on **2d,e**, as measured by the consumption of 2-bromopropene, are noticeably lower than those of **2a–c**. Moreover, in contrast to the high selectivity of catalysts based on **2a–c**, those employing **2d,e** show exceptionally poor selectivity and both form significant amounts of isomerization (V) and homocoupled (VI) byproduct (Table 7 and Figure 8). The disparate selectivities of these catalysts was surprising and somewhat unexpected, since diphosphines **2a–e** all

form catalysts that are highly selective for the Grignard cross-coupling of bromobenzene.

The most striking difference between NUPHOS derivatives that are highly selective for the formation of 2,3-dimethylpentene and those that generate significant amounts of byproduct is the structure of the 1,3-diene tether. NUPHOS derivatives that form highly selective catalysts contain a conformationally flexible acyclic 1,3-butadiene tether, while those that form catalysts that generate large amounts of byproduct contain a 1,3-diene tether formed from two exocyclic double bonds of a cyclohexane ring. This trend is further supported by the poor selectivity of catalysts based on **2f,g** (Chart 2), which have been prepared as part of a continuing program to develop and evaluate chiral versions of NUPHOS. The 1,3-butadiene tethers of these NUPHOS derivatives bear a clear structural similarity to those of **2d,e**, in that they are comprised of adjacent exocyclic double bonds on a cyclohexane ring. Most importantly, the selectivity of catalysts based on **2f,g** parallels that

Chart 2

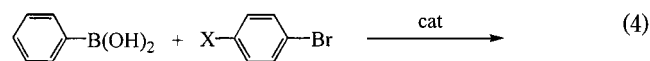


obtained with **2d,e**, all of which form significant amounts of 2-methyl-1-hexene and 2,3-dimethylbutadiene. The disparate performance of these catalyst systems is clearly illustrated in Figure 8, which compares catalyst selectivity as a function of diphosphine.

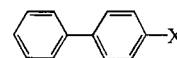
The precise origin of this dramatic change in selectivity is unclear, since **2a–e** all form catalysts that are highly selective for the cross-coupling of bromobenzene: that is, the selectivity is clearly dependent on the nature of the substrate. We believe that the difference in the 1,3-diene tethers of **2a–c** and **2d–g** most likely manifests itself in the conformational flexibility of the diphosphine, the former being considerably more flexible than the latter, the C2–C3 bond of which is constrained in a cyclohexane ring. Thus, one possible explanation for the different selectivities of these catalysts could involve the accessible range of bite angles for NUPHOS derivatives and the role of this flexibility in stabilizing and/or influencing the structure of catalytic intermediates. Kamer has related the formation of *n*-butylbenzene and biphenyl in the cross-coupling of bromobenzene to an increasing tendency to form trigonal-bipyramidal intermediates of the type [(diphosphine)Pd(H)(2-Bu)R] (**VII**) and [(diphosphine)Pd(R)<sub>2</sub>(*sec*-Bu)] (**IX**) with increasing natural bite angle (Scheme 6). However, any explanation used to account for the selectivity of NUPHOS-based catalysts may not be as straightforward as that presented by Kamer for several reasons. First, diphosphines **2d–g** are unlikely to have sufficient flexibility to increase their bite angle to the range required to stabilize five-coordinate intermediates of the type shown in Scheme 6, which is close to 110°, assuming that the diphosphine coordinates in an equatorial–equatorial manner and not axial–equatorial. Second, any explanation for the observed selectivity must also account for the marked dependence on the nature of the substrate in addition to the type of four-carbon tether. Thus, the influence of the substrate on the formation and/or fate of catalytic intermediates as well as the possible effect of changes in natural bite angle on their stability must be considered.

**Suzuki Cross-Coupling Reactions of Aryl Bromides.** The palladium-catalyzed coupling of aryl halides with organoboron reagents is an effective method for the formation of C(sp<sup>2</sup>)–C(sp<sup>2</sup>) bonds, which offers immense potential in many areas of organic synthesis.<sup>45</sup> Intense interest in this area has resulted in a number of recent noteworthy developments, including the discovery that electron-rich dialkyl- and trialkylphosphines

form catalysts that are highly active for the low-temperature Suzuki coupling of aryl chlorides and bromides.<sup>46</sup> Since the methodology outlined in Scheme 1 could be applied to the preparation of electron-rich diphosphines by quenching the organocopper intermediate with R<sub>2</sub>PCl (R = alkyl), we thought it worthwhile to examine the efficiency of diphosphines **2a–e** in the palladium-catalyzed Suzuki coupling reactions of aryl bromides. Preliminary studies have been restricted to the Pd<sub>2</sub>(dba)<sub>3</sub>/**2a–e**-catalyzed coupling of bromobenzene and the electronically activated 4-bromoacetophenone with phenylboronic acid (eq 4), the results of which are



X = H, C(O)Me



summarized in Table 7. It is well known that the efficiency of palladium-catalyzed Suzuki coupling reactions depends on a large number of variables, including the palladium source, additives, solvents, temperature, and base. However, because there is no generality to the protocol, we have not made any attempt to optimize reaction conditions but have relied on using a standard set of reaction conditions. As expected, catalysts based on **2a–e** are more efficient at cross-coupling the electronically activated 4-bromoacetophenone than bromobenzene. The results shown in Table 7 demonstrate that the efficiency of catalysts supported by NUPHOS derivatives **2a–e** compare favorably with those obtained using BINAP and dppf. In contrast to the Grignard cross-coupling reactions, which showed a dramatic dependence of catalyst performance on the nature of the four-carbon tether, the efficiency of **2a–e** in palladium-catalyzed Suzuki cross-coupling reactions appear to be largely independent of this variable.

Studies at low catalyst concentration were undertaken to minimize the amount of catalyst. In all cases reactions of 4-bromoacetophenone proceeded to near completion with 0.0001 mol % Pd, giving TON values close to 1 000 000 (mol of product) (mol of cat.)<sup>–1</sup> at 80 °C in ca. 20 h. High turnover numbers for Suzuki cross-coupling reactions are now commonplace, with early reports describing the use of cyclometalated tris(2-methylphenyl)phosphine and tris(2,4-di-*tert*-butylphenyl) phosphite palladium complexes for the cross-coupling of aryl bromides with TON of 74 000 and 1 000 000 (mol of product) (mol of cat.)<sup>–1</sup>, respectively.<sup>47</sup> More recently, Buchwald has reproducibly obtained a TON value of 10 000 000 (mol of product) (mol of cat.)<sup>–1</sup> for the cross-coupling of 4-bromoacetophenone with phenylboronic

(45) (a) Suzuki, A. In *Metal-Catalyzed Cross-Coupling Reactions*; Diedrich, F., Stang, P. J., Eds.; Wiley-VCH: Weinheim, Germany, 1998; Chapter 2. (b) Sturmer, R. *Angew. Chem., Int. Ed.* **1999**, *28*, 3307. (c) Miyaoura, N.; Suzuki, A. *Chem. Rev.* **1995**, *95*, 2457. (d) Suzuki, A. *J. Organomet. Chem.* **1999**, *576*, 147. (e) Miyaoura, N. In *Advances in Metal-Organic Chemistry*; Liebeskind, L. S., Ed.; JAI: London, 1998; Vol. 6, pp 187–243. (f) Stenforth, S. P. *Tetrahedron* **1998**, *54*, 263.

(46) (a) Wolfe, J. P.; Singer, R. A.; Yang, B. H.; Buchwald, S. L. *J. Am. Chem. Soc.* **1999**, *121*, 9550. (b) Wolfe, J. P.; Buchwald, S. L. *Angew. Chem., Int. Ed.* **1999**, *38*, 2413. (c) Old, D. W.; Wolfe, J.; Buchwald, S. L. *J. Am. Chem. Soc.* **1998**, *120*, 9722. (d) Littke, A. F.; Fu, G. C. *Angew. Chem., Int. Ed.* **1998**, *37*, 3387. (e) Littke, A. F.; Dai, C.; Fu, G. C. *J. Am. Chem. Soc.* **2000**, *122*, 4020. (f) Bei, X.; Crevier, T.; Guram, A. S.; Jandeleit, B.; Powers, T. S.; Turner, H. W.; Uno, T.; Weinberg, W. H. *Tetrahedron Lett.* **1999**, *40*, 3855.

(47) (a) Beller, M.; Fischer, H.; Hermann, W. A.; Ofelen, K.; Brossmer, *Angew. Chem., Int. Ed. Engl.* **1995**, *34*, 1848. (b) Albißson, D. A.; Bedford, R. B.; Lawrence, S.; Scully, P. N. *Chem. Commun.* **1998**, 2095.



acid in <24 h at 100 °C using a (*o*-biphenyl)P(<sup>t</sup>Bu)<sub>2</sub> catalyst system and Mathey has reported that octaethyldiphosphaferrocene is an excellent ligand for this Suzuki cross-coupling, giving a TON of 980 000 (mol of product) (mol of cat.)<sup>-1</sup> at 100 °C, which compares favorably with those obtained using **2a–e**.<sup>48</sup> The encouraging performance of catalysts based on **2a–e** suggests that catalytic asymmetric Suzuki couplings using chiral versions of NUPHOS are a worthwhile target.

In summary, the zirconium-mediated inter- and intramolecular coupling of internal alkynes and diynes has been used to prepare an entirely new class of 1,3-butadiene bridged diphosphine, by treating the resulting zirconacyclopentadiene with chlorodiphenylphosphine in the presence of copper chloride. Palladium catalysts based on NUPHOS derivatives **2a–e** are highly effective for the Grignard cross-coupling of bromobenzene with *sec*-butylmagnesium bromide and give exclusively *sec*-butylbenzene. The activity of catalysts based on 1,2,3,4-Ph<sub>4</sub>-NUPHOS is particularly impressive, and the initial TOF of 6900 (mol of product) (mol of cat.)<sup>-1</sup> h<sup>-1</sup> is more than 30 times greater than that of the most active catalyst reported to date for this coupling. In contrast, the activity and selectivity of the palladium-catalyzed coupling of 2-bromopropene depends markedly on the nature of the 1,3-diene tether of the NUPHOS derivative, those based on an acyclic 1,3-diene forming catalysts that are highly selective for the *sec*-butylated product, while those that incorporate a fused cyclohexane ring form catalysts that generate significant amounts of *n*-butylated and homocoupled byproduct. On the basis of the distinctive structural differences between these two types of NUPHOS derivatives, we believe that the accessible range of bite angles, i.e., ligand flexibility, could influence the activity and selectivity of NUPHOS-based catalysts. Although NUPHOS derivatives **2a–e** form catalysts that either rival or outperform those based on more familiar diphosphines, such as dppe, BINAP, BIPHEP, and dppf, delineation of the factors that influence catalyst selectivity and activity is not straightforward. However, even at this early stage it is clear that the activity and selectivity of NUPHOS-based catalysts is unlikely to be determined solely by the natural bite angle of the diphosphine, as this parameter varies only slightly and is close to 90°. NUPHOS derivatives **2a–e** and Pd<sub>2</sub>(dba)<sub>3</sub> also form highly effective catalysts for the Suzuki coupling of aryl bromides and phenylboronic acid, and at low catalyst loading TON values of 1 000 000 (mol of product) (mol of cat.)<sup>-1</sup> have been achieved. Since the results of our preliminary catalytic studies have proven to be highly encouraging, the effectiveness of this new class of diphosphine for a range of palladium-catalyzed reactions, detailed mechanistic investigations to determine the factors that influence/determine catalyst activity and selectivity, and the synthesis of chiral versions of NUPHOS and their applications in asymmetric transformations are currently underway.

## Experimental Section

**General Procedures.** All manipulations involving air-sensitive materials were carried out in an inert-atmosphere

glovebox or using standard Schlenk line techniques under an atmosphere of nitrogen or argon in oven-dried glassware. Diethyl ether and hexane were distilled from potassium/sodium alloy, tetrahydrofuran from potassium, dichloromethane from calcium hydride, and methanol from magnesium. Unless otherwise stated, commercially purchased materials were purchased and used without further purification. Bis(cyclopentadienyl)zirconium dichloride, diphenylacetylene, but-2-yne, 1-phenylpropyne, butyllithium, copper(I) chloride, phenylboronic acid, 4-bromoacetophenone, sodium carbonate, and tris(dibenzylideneacetone)dipalladium were purchased from Aldrich Chemical Co., and 3,9-dodecadiyne was purchased from Acros Chemicals. Deuteriochloroform was predried with calcium hydride, vacuum-transferred, and stored over 4 Å molecular sieves. <sup>1</sup>H and <sup>31</sup>P{<sup>1</sup>H} and <sup>13</sup>C{<sup>1</sup>H} NMR spectra were recorded on a JEOL LAMBDA 500 or Bruker AC 200, AMX 300, and DRX 500 machines. GC analyses were conducted on a Varian CP3800 connected to a Varian C8400 auto sampler or a Perkin-Elmer 8700 gas chromatograph. Response factors were determined by injection of samples containing known quantities of authentic sample. The palladium and platinum complexes [(cycloocta-1,5-diene)MCl<sub>2</sub>] (M = Pd, Pt)<sup>49,50</sup> and 1,8-diphenyloctadiyne<sup>51</sup> were prepared as previously described.

**Synthesis of 1,4-Bis(diphenylphosphino)-1,2,3,4-tetraphenyl-1,3-butadiene (2a).** A Schlenk flask charged with Cp<sub>2</sub>ZrCl<sub>2</sub> (4.10 g, 14.0 mmol), diphenylacetylene (5.0 g, 28.0 mmol), and THF (30 mL) was cooled to -78 °C, and *n*BuLi in hexane (11.2 mL, 2.5 M, 28.0 mmol) was added with rapid stirring. The solution was stirred for 20 min, after which time it was warmed to room temperature and stirred for a further 2.5 h. The solution was then cooled to 0 °C, CuCl (2.8 g, 28.0 mmol) was added, and the reaction mixture was stirred for 20–30 min, after which time a solution of PPh<sub>2</sub>Cl (5.0 mL, 28.0 mmol) in THF (15 mL) was added, while the reaction mixture was maintained at 0 °C. The solution was stirred overnight and filtered and the solvent removed under reduced pressure to give a deep orange crystalline solid (<sup>31</sup>P{<sup>1</sup>H} NMR -5.1 ppm, br s). The solid was dissolved in CH<sub>2</sub>Cl<sub>2</sub>, the solution was washed with water (3 × 10 mL) and extracted with aqueous ammonia (3 × 60 mL), the extracts were separated, dried over magnesium sulfate, and filtered, and the solvent was removed to leave a yellow crystalline solid. Crystallization by slow diffusion of *n*-hexane into a toluene solution at room temperature gave **2a** in 44% yield (4.4 g). <sup>31</sup>P{<sup>1</sup>H} NMR (202.0 MHz, CDCl<sub>3</sub>, δ): 1.1 (s, PPh<sub>2</sub>). <sup>1</sup>H NMR (500.0 MHz, CDCl<sub>3</sub>, δ): 7.4 (td, *J* = 6.4 Hz, 1.5 Hz, C<sub>6</sub>H<sub>5</sub>), 7.31–7.35 (m, C<sub>6</sub>H<sub>5</sub>), 6.96–7.04 (m, C<sub>6</sub>H<sub>5</sub>), 6.87 (t, *J* = 7.0 Hz, C<sub>6</sub>H<sub>5</sub>), 6.74 (t, *J* = 8.2 Hz, C<sub>6</sub>H<sub>5</sub>), 6.61 (t, *J* = 7.3 Hz, C<sub>6</sub>H<sub>5</sub>). <sup>13</sup>C{<sup>1</sup>H} NMR (125.65 MHz, CDCl<sub>3</sub>, δ): 157.5 (dd, *J*<sub>PC</sub> = 7.5, 40.3 Hz, C<sub>6</sub>H<sub>5</sub>), 143.2 (d, *J*<sub>PC</sub> = 13.4 Hz, C<sub>6</sub>H<sub>5</sub>), 140.8 (s, C<sub>6</sub>H<sub>5</sub>), 139.1 (dd, *J*<sub>PC</sub> = 20.6, 4.1 Hz, C<sub>6</sub>H<sub>5</sub>), 137.6 (d, *J*<sub>PC</sub> = 12.2 Hz, C<sub>6</sub>H<sub>5</sub>), 135.4 (d, *J*<sub>PC</sub> = 14.5 Hz, C<sub>6</sub>H<sub>5</sub>), 134.3 (d, *J*<sub>PC</sub> = 21.6 Hz, C<sub>6</sub>H<sub>5</sub>), 132.5 (d, *J*<sub>PC</sub> = 16.5 Hz, C<sub>6</sub>H<sub>5</sub>), 131.5 (s, C<sub>6</sub>H<sub>5</sub>), 129.7 (s, C<sub>6</sub>H<sub>5</sub>), 128.3 (s, C<sub>6</sub>H<sub>5</sub>), 127.6 (s, C<sub>6</sub>H<sub>5</sub>), 127.5 (s, C<sub>6</sub>H<sub>5</sub>), 127.4 (s, C<sub>6</sub>H<sub>5</sub>), 127.3 (s, C<sub>6</sub>H<sub>5</sub>), 217.2 (s, C<sub>6</sub>H<sub>5</sub>), 216.7 (s, C<sub>6</sub>H<sub>5</sub>), 125.8 (s, C<sub>6</sub>H<sub>5</sub>). Anal. Calcd for C<sub>52</sub>H<sub>40</sub>P<sub>2</sub>: C, 85.92; H, 5.55. Found: C, 85.55; H, 5.42.

**Synthesis of 1,4-Bis(diphenylphosphino)-1,2,3,4-tetramethyl-1,3-butadiene (2b).** Compound **2b** was prepared according to the procedure described above and was isolated as yellow crystals in 55% yield by slow diffusion of a chloroform solution layered with methanol. <sup>31</sup>P{<sup>1</sup>H} NMR (121.5 MHz, CDCl<sub>3</sub>, δ): -4.2 (s, PPh<sub>2</sub>). <sup>1</sup>H NMR (500.0 MHz, CDCl<sub>3</sub>, δ): 7.33 (t, *J* = 7.0 Hz, C<sub>6</sub>H<sub>5</sub>), 7.2–7.25 (m, C<sub>6</sub>H<sub>5</sub>), 6.96–7.10 (m, C<sub>6</sub>H<sub>5</sub>), 2.20 (s, 6H, CH<sub>3</sub>), 1.58 (s, 6H, CH<sub>3</sub>). <sup>13</sup>C{<sup>1</sup>H} NMR (125.65 MHz, CDCl<sub>3</sub>, δ): 155.2 (dd, *J*<sub>PC</sub> = 10.4 Hz, 39.3, C<sub>6</sub>H<sub>5</sub>), 138.4 (d, *J*<sub>PC</sub> = 14.5 Hz, C=C), 136.9 (d, *J*<sub>PC</sub> = 12.3 Hz, C<sub>6</sub>H<sub>5</sub>), 133.1

(49) Drew, D.; Doyle, J. R. *Inorg. Synth.* **1990**, *28*, 348.

(50) Drew, D.; Doyle, J. R. *Inorg. Synth.* **1990**, *28*, 346.

(51) Lucht, B. L.; Mao, S. S. H.; Tilley, T. D. *J. Am. Chem. Soc.* **1998**, *120*, 4354.

(48) Sava, X.; Ricard, L.; Mathey, F.; Le Floch, P. *Organometallics* **2000**, *19*, 4899.

(d,  $J_{\text{PC}} = 16.5$  Hz,  $\text{C}_6\text{H}_5$ ), 132.4 (d,  $J_{\text{PC}} = 19.0$  Hz,  $\text{C}_6\text{H}_5$ ), 128.1 (d,  $J_{\text{PC}} = 5.2$  Hz,  $\text{C}_6\text{H}_5$ ), 127.9 (s,  $\text{C}_6\text{H}_5$ ), 127.7 (d,  $J_{\text{PC}} = 5.2$  Hz,  $\text{C}_6\text{H}_5$ ), 127.2 (s,  $\text{C}_6\text{H}_5$ ), 125.5 (d,  $J_{\text{PC}} = 7.3$  Hz,  $\text{C}=\text{C}$ ), 21.9 (t,  $J_{\text{PC}} = 9.3$  Hz,  $\text{CH}_3$ ), 16.2 (d,  $J_{\text{PC}} = 4.1$  Hz,  $\text{CH}_3$ ). Anal. Calcd for  $\text{C}_{32}\text{H}_{32}\text{P}_2$ : C, 80.31; H, 6.73. Found: C, 79.99; H, 6.67.

**Synthesis of 1,4-Bis(diphenylphosphino)-1,3-diphenyl-2,4-dimethyl-1,3-butadiene (2c).** Compound **2c** was prepared according to the procedure described above for **2a** and isolated as colorless crystals in 66% yield by slow diffusion of a chloroform solution layered with hexane.  $^{31}\text{P}\{^1\text{H}\}$  NMR (121.5 MHz,  $\text{CDCl}_3$ ,  $\delta$ ): -2.4 (s,  $\text{PPh}_2$ ), -6.4 (s,  $\text{PPh}_2$ ).  $^1\text{H}$  NMR (500.0 MHz,  $\text{CDCl}_3$ ,  $\delta$ ): 6.75–7.45 (m,  $\text{C}_6\text{H}_5$ , 28H), 6.5 (d,  $J = 6.7$  Hz, 2H), 2.02 (s, 3H,  $\text{CH}_3$ ), 1.60 (dd,  $J_{\text{PH}} = 3.1$  Hz,  $J_{\text{PH}} = 1.3$  Hz, 3H,  $\text{CH}_3$ ).  $^{13}\text{C}\{^1\text{H}\}$  NMR (75.4 MHz,  $\text{CDCl}_3$ ,  $\delta$ ): 140.9–124.5 (m,  $\text{C}_6\text{H}_5$ ,  $\text{C}=\text{C}$ ), 25.1 (t,  $J_{\text{PC}} = 8.1$  Hz,  $\text{CH}_3$ ), 17.26 (d,  $J_{\text{PC}} = 3.8$  Hz,  $\text{CH}_3$ ). Anal. Calcd for  $\text{C}_{42}\text{H}_{36}\text{P}_2$ : C, 83.69; H, 6.02. Found: C, 83.99; H, 6.37.

**Synthesis of 1,2-bis(1-(diphenylphosphino)prop-1-ylidene)cyclohexane (2d).** To a Schlenk flask charged with  $\text{Cp}_2\text{ZrCl}_2$  (5.40 g, 18.4 mmol), 3,9-dodecadiyne (3.6 mL, 3.0 g, 18.4 mmol), and THF (50 mL), cooled to  $-78^\circ\text{C}$ , was added  $n\text{BuLi}$  (14.0 mL, 2.5 M, 35.0 mmol) with rapid stirring. The solution was stirred for 20 min, after which time it was warmed to room temperature and stirred for a further 2.5 h. The solution was then cooled to  $0^\circ\text{C}$ ,  $\text{CuCl}$  (3.60 g, 36.3 mmol) was added, and the reaction mixture was stirred for 20–30 min, after which time a solution of  $\text{PPh}_2\text{Cl}$  (6.77 mL, 37.0 mmol) in THF (15 mL) was added, while the reaction mixture was maintained at  $0^\circ\text{C}$ . The solution was stirred overnight and filtered and the solvent removed under reduced pressure to give a deep orange crystalline solid. The solid was extracted with 150 mL of a diethyl ether/tetrahydrofuran mixture (v/v, 5:1), washed with water ( $3 \times 10$  mL), extracted with 80% ethylenediamine ( $3 \times 60$  mL), separated, dried over magnesium sulfate, and filtered and the solvent removed to leave a yellow crystalline solid. Crystallization by slow diffusion of *n*-hexane into a toluene solution at room temperature gave **2d** in 26% yield (2.60 g). X-ray-quality crystals of the intermediate copper complex **1d** were grown by slow diffusion of methanol into a chloroform solution at room temperature prior to washing the crude filtrate with 1,2-ethylenediamine solution. Compound **1d**:  $^1\text{P}\{^1\text{H}\}$  NMR (121.5 MHz,  $\text{CDCl}_3$ ,  $\delta$ ) -3.0 (s,  $\text{PPh}_2$ );  $^1\text{H}$  NMR (500.0 MHz,  $\text{CDCl}_3$ ,  $\delta$ ) 7.77 (q,  $J = 5.8$  Hz, 4H,  $\text{C}_6\text{H}_5$ ), 7.69 (m, 4H,  $\text{C}_6\text{H}_5$ ), 7.16–7.36 (m, 12H,  $\text{C}_6\text{H}_5$ ), 2.20 (d,  $J = 9.4$  Hz, 2H,  $\text{C}_6\text{H}_5$ ), 1.76 (m, 2H,  $\text{C}_6\text{H}_5$ ), 1.67 (br, 2H,  $\text{C}_6\text{H}_5$ ), 1.49 (m, 2H,  $\text{C}_6\text{H}_5$ ), 1.30 (br, 4H,  $\text{CH}_2\text{CH}_3$ ), 0.37 (t,  $J = 7.6$  Hz, 6H,  $\text{CH}_2\text{CH}_3$ ). Compound **2d**:  $^{31}\text{P}\{^1\text{H}\}$  NMR (121.5 MHz,  $\text{CDCl}_3$ ,  $\delta$ ) -5.5 (s,  $\text{PPh}_2$ );  $^1\text{H}$  NMR (500.0 MHz,  $\text{CDCl}_3$ ,  $\delta$ ) 7.00–7.75 (m,  $\text{C}_6\text{H}_5$ , 20H), 2.8 (d,  $J = 11.3$  Hz, 2H,  $\text{cy CH}_2$ ), 2.21 (m, 4H,  $\text{CH}_2\text{CH}_3$ ), 1.9 (br, 2H,  $\text{cy CH}_2$ ), 1.50 (br t, 2H,  $\text{cy CH}_2$ ), 1.2 (br, 2H,  $\text{cy CH}_2$ ), 0.35 (t,  $J = 5.8$  Hz, 6H,  $\text{CH}_2\text{CH}_3$ );  $^{13}\text{C}\{^1\text{H}\}$  NMR (75.4 MHz,  $\text{CDCl}_3$ ,  $\delta$ ) 139.4–127.3 (m,  $\text{C}_6\text{H}_5$ ,  $\text{C}=\text{C}$ ), 35.7 (t,  $J_{\text{PC}} = 5.1$  Hz,  $\text{cy-CH}_2$ ), 28.9 (s,  $\text{cy-CH}_2$ ), 23.7 (s,  $\text{CH}_2\text{CH}_3$ ), 14.4 (s,  $\text{CH}_2\text{CH}_3$ ). Anal. Calcd for  $\text{C}_{36}\text{H}_{38}\text{P}_2$ : C, 81.17; H, 7.19. Found: C, 80.91; H, 7.01.

**Synthesis of 1,2-bis(1-(diphenylphosphino)benzylidene)cyclohexane (2e).** 1,2-Bis(((diphenylphosphino)phenyl)methylene)cyclohexane was isolated in 37% yield according to the procedure described above for **2d**.  $^{31}\text{P}\{^1\text{H}\}$  NMR (121.5 MHz,  $\text{CDCl}_3$ ,  $\delta$ ): 1.2 (s,  $\text{PPh}_2$ ).  $^1\text{H}$  NMR (500.0 MHz,  $\text{CDCl}_3$ ,  $\delta$ ): 6.70–7.60 (m, 30H,  $\text{C}_6\text{H}_5$ ), 2.45 (br d,  $J = 12.1$  Hz, 2H,  $\text{cy CH}_2$ ), 1.90 (td,  $J = 8.9$  Hz,  $J = 3.7$  Hz, 2H,  $\text{cy CH}_2$ ), 1.7 (br, 2H,  $\text{cy CH}_2$ ), 1.48 (t,  $J = 9.5$  Hz,  $\text{CH}_2$ ,  $\text{cy CH}_2$ ). Anal. Calcd for  $\text{C}_{44}\text{H}_{38}\text{P}_2$ : C, 84.05; H, 6.09. Found: C, 84.44; H, 6.01.

**Dichloro[1,4-bis(diphenylphosphino)-1,2,3,4-tetraphenyl-1,3-butadiene]palladium (3a).** A solution of [(cycloocta-1,5-diene) $\text{PdCl}_2$ ] (0.25 g, 0.88 mmol) in dichloromethane (8–10 mL) was treated with a dichloromethane solution (7–10 mL) of **1a** (0.64 g, 0.88 mmol) and stirred vigorously for ca. 1–2 h. The reaction mixture was filtered and the solvent removed to leave a yellow solid residue. Crystallization by slow

diffusion of *n*-hexane into a dichloromethane solution at room temperature gave **2a** as deep red prisms in 85% yield (0.70 g).  $^{31}\text{P}\{^1\text{H}\}$  NMR (121.4 MHz,  $\text{CDCl}_3$ ,  $\delta$ ): 19.6 (s,  $\text{PPh}_2$ ).  $^1\text{H}$  NMR (500.0 MHz,  $\text{CDCl}_3$ , 193 K,  $\delta$ ): 9.57 (br, 2H,  $\text{C}_6\text{H}_5$ ), 8.41 (br t, 2H,  $\text{C}_6\text{H}_5$ ), 8.01 (br, 6H,  $\text{C}_6\text{H}_5$ ), 6.76–7.12 (m, 14H,  $\text{C}_6\text{H}_5$ ), 6.66 (t,  $J = 7.3$  Hz, 2H,  $\text{C}_6\text{H}_5$ ), 6.63 (t,  $J = 7.2$  Hz, 4H,  $\text{C}_6\text{H}_5$ ), 6.51 (t,  $J = 7.3$  Hz, 2H,  $\text{C}_6\text{H}_5$ ), 6.18 (d,  $J = 7.6$  Hz, 4H,  $\text{C}_6\text{H}_5$ ), 6.06 (d,  $J = 7.6$  Hz, 2H,  $\text{C}_6\text{H}_5$ ), 5.94 (d,  $J = 7.6$  Hz, 2H,  $\text{C}_6\text{H}_5$ ). Anal. Calcd for  $\text{C}_{52}\text{H}_{40}\text{P}_2\text{PdCl}_2 \cdot \text{CH}_2\text{Cl}_2$ : C, 64.43; H, 4.25. Found: C, 64.20; H, 4.28.

**Dichloro[1,4-bis(diphenylphosphino)-1,2,3,4-tetramethyl-1,3-butadiene]palladium (3b).** Compound **2b** was prepared according to the procedure described above for **4a** and was isolated as yellow crystals in 78% yield by slow diffusion of diethyl ether into a chloroform solution layered at room temperature.  $^{31}\text{P}\{^1\text{H}\}$  NMR (121.4 MHz,  $\text{CDCl}_3$ ,  $\delta$ ): 24.0 (s,  $\text{PPh}_2$ ).  $^1\text{H}$  NMR (500.0 MHz,  $\text{CDCl}_3$ ,  $\delta$ ): 8.30 (br,  $\text{C}_6\text{H}_5$ ), 7.50–7.57 (m,  $\text{C}_6\text{H}_5$ ), 7.15–7.27 (m,  $\text{C}_6\text{H}_5$ ), 1.20 (d,  $J = 12.5$  Hz, 6H,  $\text{CH}_3$ ), 1.12 (s, 6H,  $\text{CH}_3$ ).  $^{13}\text{C}\{^1\text{H}\}$  NMR (125.65 MHz,  $\text{CDCl}_3$ ,  $\delta$ ): 150.7 (s,  $\text{C}_6\text{H}_5$ ), 135.7 (d,  $J_{\text{PC}} = 12.4$  Hz,  $\text{C}_6\text{H}_5$ ), 134.6 (d,  $J_{\text{PC}} = 10.3$  Hz,  $\text{C}_6\text{H}_5$ ), 131.9 (s,  $\text{C}_6\text{H}_5$ ), 130.5 (s,  $\text{C}_6\text{H}_5$ ), 130.3 (s,  $\text{C}_6\text{H}_5$ ), 129.9 (d,  $J_{\text{PC}} = 26.0$  Hz,  $\text{C}=\text{C}$ ), 128.9 (d,  $J_{\text{PC}} = 10.4$  Hz,  $\text{C}_6\text{H}_5$ ), 127.6 (s,  $\text{C}_6\text{H}_5$ ), 127.3 (d,  $J_{\text{PC}} = 40.0$  Hz,  $\text{C}=\text{C}$ ), 127.2 (s,  $\text{C}_6\text{H}_5$ ), 20.4 (d,  $J_{\text{PC}} = 6.1$  Hz,  $\text{CH}_3$ ), 18.7 (d,  $J_{\text{PC}} = 12.3$  Hz,  $\text{CH}_3$ ). Anal. Calcd for  $\text{C}_{32}\text{H}_{32}\text{P}_2\text{PdCl}_2 \cdot \text{CHCl}_3$ : C, 51.13; H, 4.29. Found: C, 51.23; H, 4.32.

**Dichloro[1,4-bis(diphenylphosphino)-1,3-diphenyl-2,4-dimethyl-1,3-butadiene]palladium (3c).** Compound **2c** was prepared according to the procedure described above for **2a** and was isolated as yellow crystals in 78% yield by slow diffusion of methanol into a chloroform or dichloromethane solution at room temperature.  $^{31}\text{P}\{^1\text{H}\}$  NMR (121.4 MHz,  $\text{CDCl}_3$ ,  $\delta$ ): 26.3 (d,  $J_{\text{PP}} = 6.1$  Hz,  $\text{PPh}_2$ ), 21.4 (d,  $J_{\text{PP}} = 6.1$  Hz,  $\text{PPh}_2$ ).  $^1\text{H}$  NMR (500.0 MHz,  $\text{CDCl}_3$ ,  $\delta$ ): 8.65 (m br, 4H,  $\text{C}_6\text{H}_5$ ), 6.80–7.50 (m, 24H,  $\text{C}_6\text{H}_5$ ), 6.75 (dt,  $J = 2.8$  Hz, 7.6 Hz, 2H,  $\text{C}_6\text{H}_5$ ), 1.20 (d,  $J = 12.5$  Hz, 6H,  $\text{CH}_3$ ), 0.77 (br, 6H,  $\text{CH}_3$ ). Anal. Calcd for  $\text{C}_{42}\text{H}_{36}\text{P}_2\text{PdCl}_2 \cdot \text{CH}_2\text{Cl}_2$ : C, 59.72; H, 4.42. Found: C, 59.93; H, 4.21.

**Dichloro[1,2-bis((diphenylphosphino)ethylmethylene)cyclohexane]palladium (3d).** Compound **2d** was prepared according to the procedure described above for **2a** and was isolated as yellow crystals in 78% yield by slow diffusion of methanol into a chloroform solution at room temperature.  $^{31}\text{P}\{^1\text{H}\}$  NMR (121.4 MHz,  $\text{CDCl}_3$ ,  $\delta$ ): 21.5 (s,  $\text{PPh}_2$ ).  $^1\text{H}$  NMR (500.0 MHz,  $\text{CDCl}_3$ ,  $\delta$ ): 8.3 (br, 4H,  $\text{C}_6\text{H}_5$ ), 7.57 (m, 16H,  $\text{C}_6\text{H}_5$ ), 2.2 (d,  $J = 10.4$  Hz, 2H,  $\text{cy CH}_2$ ), 2.08 (8 line multiplet, 2H,  $\text{CH}_2\text{CH}_3$ ), 1.57 (br, 2H,  $\text{cy CH}_2$ ), 1.51 (m, 2H,  $\text{CH}_2\text{CH}_3$ ), 1.18 (br, 4H,  $\text{cy CH}_2$ ), 0.21 (br t,  $J = 7.0$  Hz, 6H,  $\text{CH}_2\text{CH}_3$ ).  $^{13}\text{C}\{^1\text{H}\}$  NMR (125.65 MHz,  $\text{CDCl}_3$ ,  $\delta$ ): 135.0–127.2 (m,  $\text{C}_6\text{H}_5$ ,  $\text{C}=\text{C}$ ), 34.2 (s,  $\text{cy CH}_2$ ), 26.9 (s,  $\text{cy CH}_2$ ), 24.1 (s,  $\text{CH}_2\text{CH}_3$ ), 12.8 (s,  $\text{CH}_2\text{CH}_3$ ). Anal. Calcd for  $\text{C}_{36}\text{H}_{38}\text{P}_2\text{PdCl}_2$ : C, 60.93; H, 5.40. Found: C, 60.43; H, 4.91.

**Dichloro[1,2-bis((diphenylphosphino)phenylmethylene)cyclohexane]palladium (3e).** Compound **2d** was prepared according to the procedure described above for **2a** and was isolated as yellow crystals in 76% yield by slow diffusion of methanol into a chloroform solution at room temperature.  $^{31}\text{P}\{^1\text{H}\}$  NMR (121.4 MHz,  $\text{CDCl}_3$ ,  $\delta$ ): 18.9 (s,  $\text{PPh}_2$ ).  $^1\text{H}$  NMR (500.0 MHz,  $\text{CDCl}_3$ ,  $\delta$ ): 8.69 (br, 4H,  $\text{C}_6\text{H}_5$ ), 7.57 (br, 8H,  $\text{C}_6\text{H}_5$ ), 6.74–7.4 (m, 8H,  $\text{C}_6\text{H}_5$ ), 6.60 (t,  $J = 7.0$  Hz, 2H,  $\text{C}_6\text{H}_5$ ), 6.23 (br s, 4H,  $\text{C}_6\text{H}_5$ ), 6.19 (d,  $J = 7.6$  Hz, 2H,  $\text{C}_6\text{H}_5$ ), 5.89 (d,  $J = 7.6$  Hz, 2H,  $\text{C}_6\text{H}_5$ ), 2.82 (d,  $J = 11.9$  Hz, 2H,  $\text{cy CH}_2$ ), 2.48 (d,  $J = 9.45$  Hz, 2H,  $\text{cy CH}_2$ ), 1.98 (br d,  $J = 12.8$  Hz, 2H,  $\text{cy CH}_2$ ), 1.50 (br s, 2H,  $\text{cy CH}_2$ ). Anal. Calcd for  $\text{C}_{44}\text{H}_{38}\text{P}_2\text{PdCl}_2$ : C, 65.59; H, 4.75. Found: C, 65.88; H, 4.97.

**Dichloro[1,2-bis((diphenylphosphino)phenylmethylene)cyclohexane]platinum (4e).** A solution of [(cycloocta-1,5-diene) $\text{PtCl}_2$ ] (0.400 g, 1.07 mmol) in dichloromethane (20 mL) was treated with a dichloromethane solution (10 mL) of **1e** (0.67 g, 1.07 mmol) and stirred vigorously for ca. 12 h. The reaction mixture was filtered and the solvent removed to

**Table 8.** Summary of Crystal Data and Structure Determination for Compounds **1d**, **2a**, **3b,c** and **4e**

	<b>1d</b>	<b>2a</b>	<b>3b</b>	<b>3c</b>	<b>4e</b>
formula	C <sub>52</sub> H <sub>40</sub> P <sub>2</sub>	C <sub>72</sub> H <sub>76</sub> Cl <sub>2</sub> Cu <sub>2</sub> P <sub>4</sub> · 2CH <sub>3</sub> OH·2CHCl <sub>3</sub>	C <sub>32</sub> H <sub>32</sub> Cl <sub>2</sub> P <sub>2</sub> Pd· CHCl <sub>3</sub>	C <sub>42</sub> H <sub>36</sub> Cl <sub>2</sub> P <sub>2</sub> Pd· CH <sub>2</sub> Cl <sub>2</sub>	C <sub>44</sub> H <sub>38</sub> Cl <sub>2</sub> P <sub>2</sub> Pt· 4CHCl <sub>3</sub>
<i>M<sub>r</sub></i>	726.8	1566.0	775.2	864.9	1372.2
color	colorless	yellow	yellow	red	colorless
temp, K	160	160	160	160	153
cryst syst	monoclinic	monoclinic	monoclinic	monoclinic	monoclinic
space group	<i>C2/c</i>	<i>C2/c</i>	<i>P2<sub>1</sub>/c</i>	<i>P2<sub>1</sub>/c</i>	<i>P2<sub>1</sub>/n</i>
<i>a</i> , Å	17.3356(9)	29.012(2)	12.7882(7)	10.2320(8)	10.762(2)
<i>b</i> , Å	10.1305(5)	10.1870(7)	16.2276(9)	35.194(3)	21.866(4)
<i>c</i> , Å	22.8891(12)	26.5126(19)	16.8847(10)	11.4065(8)	23.807(5)
β, deg	97.829(1)	108.923(2)	108.070(1)	108.964(11)	101.978(3)
<i>V</i> , Å <sup>3</sup>	3982.3(4)	7412.1(9)	3331.1(3)	3884.6(5)	5480.7(18)
<i>Z</i>	4	4	4	4	4
μ, cm <sup>-1</sup>	1.45	9.94	10.77	8.66	33.35
θ <sub>max</sub> , deg	28.7	28.5	28.5	28.5	28.6
no. of rflns measd	16803	31062	28070	33131	26954
no. of unique rflns	4723	8796	7807	9202	12276
<i>R</i> <sub>int</sub> (on <i>F</i> <sup>2</sup> )	0.0254	0.0346	0.0232	0.0270	0.0762
no. of params	244	419	374	453	586
<i>R</i> ( <i>F</i> <sup>2</sup> > 2σ( <i>F</i> <sup>2</sup> )) <sup>a</sup>	0.0350	0.0407	0.0254	0.0401	0.0547
<i>R</i> <sub>w</sub> (all data) <sup>b</sup>	0.0953	0.1154	0.0679	0.0889	0.1238
GOF ( <i>S</i> ) <sup>c</sup>	1.050	1.046	1.068	1.074	0.888
max, min diff map, e Å <sup>-3</sup>	0.30, -0.26	1.28, -0.89	1.06, -0.97	0.67, -1.06	2.73, -1.25

<sup>a</sup> Conventional  $R = \sum ||F_o| - |F_c|| / \sum |F_o|$  for "observed" reflections having  $F_o^2 > 2\sigma(F_o^2)$ . <sup>b</sup>  $R_w = [\sum w(F_o^2 - F_c^2)^2 / \sum w(F_o^2)^2]^{1/2}$  for all data. <sup>c</sup> GOF =  $[\sum w(F_o^2 - F_c^2)^2 / ((\text{no. of unique reflections}) - (\text{no. of parameters}))]^{1/2}$ .

leave a yellow solid residue. Crystallization from a dichloromethane–chloroform mixture at room temperature gave **4e** as colorless prisms in 73% yield (0.70 g). <sup>31</sup>P{<sup>1</sup>H} NMR (121.5 MHz, CDCl<sub>3</sub>, δ): 1.2 (t, *J*<sub>PP</sub> = 3054 Hz, PPh<sub>2</sub>). <sup>1</sup>H NMR (500.0 MHz, CDCl<sub>3</sub>, δ): 8.57 (br, 4H, C<sub>6</sub>H<sub>5</sub>), 7.76 (br, 6H, C<sub>6</sub>H<sub>5</sub>), 7.0 (t, *J* = 7.5 Hz, 2H, C<sub>6</sub>H<sub>5</sub>), 6.96 (t, *J* = 7.2 Hz, 2H, C<sub>6</sub>H<sub>5</sub>), 6.89 (t, *J* = 7.4 Hz, 2H, C<sub>6</sub>H<sub>5</sub>), 6.78 (t, *J* = 7.1 Hz, 2H, C<sub>6</sub>H<sub>5</sub>), 6.75 (m, 2H, C<sub>6</sub>H<sub>5</sub>), 6.25 (t, *J* = 7.4 Hz, 2H, C<sub>6</sub>H<sub>5</sub>), 6.21 (d, *J* = 7.3 Hz, 2H, C<sub>6</sub>H<sub>5</sub>), 5.94 (t, *J* = 7.3 Hz, 2H, C<sub>6</sub>H<sub>5</sub>), 1.86 (d, *J* = 13.4 Hz, 2H, cy CH<sub>2</sub>), 1.56 (br, 2H, cy CH<sub>2</sub>), 1.47 (br, 2H, cy CH<sub>2</sub>), 1.19 (br t, *J* = 9.0 Hz, 2H, cy CH<sub>2</sub>). Anal. Calcd for C<sub>44</sub>H<sub>38</sub>Cl<sub>2</sub>Pt·4CHCl<sub>3</sub>: C, 41.99; H, 2.79. Found: C, 41.23; H, 2.33.

**Palladium-Catalyzed Cross-Couplings.** A Schlenk flask was charged with [(diphosphine)PdCl<sub>2</sub>] (16.6 μmol), *n*-decane (1.7 mL, 8.3 mmol), and bromobenzene or 2-bromopropene (16.6 mmol) under nitrogen. The solution was cooled to -78 °C, and *sec*-butylmagnesium chloride (16.6 mL, 2 M solution in *n*-hexane, 16.6 mmol) was added. The reaction mixture was warmed to room temperature with stirring and the reaction monitored by gas chromatography until the starting material had been completely consumed. Samples were hydrolyzed with 10% HCl and the ether layer separated and analyzed by gas chromatography. GC conditions: initial temperature 50 °C for 5 min, final temperature 300 °C, ramp rate 10 °C/min to 200 °C for 5 min, ramp rate 20 °C/min to 300 °C for 5 min, injection temperature 300 °C, detector temperature 300 °C, carrier gas He 20.0 psig, RTX5 capillary column, 30 m × 0.25 mm i.d.

**General Procedure for the Suzuki Coupling of Aryl Bromides.** An oven-dried Schlenk flask was evacuated, back-filled with argon, and charged with potassium carbonate (1.520 g, 11.00 mmol), phenylboronic acid (1.006 g, 8.25 mmol), 4-bromoacetophenone (1.095 g, 5.50 mmol), *n*-decane (0.5 mL, 2.37 mmol), and dioxane (2 mL). In a separate oven-dried flask, a solution of ligand (0.0034 mmol) and [Pd<sub>2</sub>(dba)<sub>3</sub>] (0.0015 g, 0.0017 mmol) in ~1 mL of dioxane was stirred for 15 min before being transferred to the reaction mixture. The flask was sealed, and the reaction mixture was stirred at 85 °C for 10

min, after which time it was cooled and diluted with diethyl ether and an aliquot extracted and filtered through Celite before being analyzed by gas chromatography. GC conditions: initial temperature 80 °C, final temperature 170 °C, ramp rate 8 °C/min, injection temperature 200 °C, detector temperature 300 °C, carrier gas He 30 mL/min, column 25 m × 0.32 mm i.d., WCOT fused silica CP-Chirasil-Dex CB stationary phase.

**Crystal Structure Determinations of 1d, 2a, 3b,c, and 4e.** All measurements were made on Bruker AXS SMART 1K CCD diffractometers using graphite-monochromated Mo Kα radiation (λ = 0.71073 Å). Further information is given in Table 8. The structures were determined and refined by standard procedures, including constrained hydrogen atoms. The programs used were Bruker AXS SMART (diffractometer control), SAINT (integration),<sup>52</sup> and SHELXTL (structure determination and graphics),<sup>53</sup> together with local programs.

**Acknowledgment.** We gratefully acknowledge funding from the Queen's University of Belfast, the EPSRC (E.G.R., P.A.C., and equipment to W.C.), and INEOS Acrylics (P.A.C.) and thank Johnson Matthey for loans of palladium salts.

**Supporting Information Available:** For **1d**, **2a**, **3b,c**, and **4e**, tables giving details of the structure determination, non-hydrogen atomic positional parameters, all bond distances and angles, anisotropic displacement parameters, and hydrogen atomic coordinates. This material is available free of charge via the Internet at <http://pubs.acs.org>. Observed and calculated structure factor tables are available from the authors upon request.

OM011049W

(52) SMART and SAINT software for CCD area detectors; Bruker AXS Inc., Madison, WI., 1997.

(53) Sheldrick, G. M. *SHELXTL Manual*; Bruker AXS: Madison, WI, 1997.